

**Evaluating ice cloud  
parameterizations in  
CAM5**

K. Zhang et al.

**Evaluating and constraining ice cloud  
parameterizations in CAM5 using aircraft  
measurements from the SPARTICUS  
campaign**

**K. Zhang<sup>1</sup>, X. Liu<sup>1</sup>, M. Wang<sup>1</sup>, J. M. Comstock<sup>1</sup>, D. L. Mitchell<sup>2</sup>, S. Mishra<sup>2,3</sup>, and  
G. G. Mace<sup>4</sup>**

<sup>1</sup>Pacific Northwest National Laboratory, Richland, WA, USA

<sup>2</sup>Desert Research Institute, Reno, NV, USA

<sup>3</sup>Cooperative Institute for Mesoscale Meteorological Studies (CIMMS), Norman, OK, USA

<sup>4</sup>University of Utah, Salt Lake City, UT, USA

Received: 21 November 2012 – Accepted: 26 December 2012 – Published: 11 January 2013

Correspondence to: K. Zhang (kai.zhang@pnnl.gov)

Published by Copernicus Publications on behalf of the European Geosciences Union.

Title Page

Abstract

Introduction

Conclusions

References

Tables

Figures

◀

▶

◀

▶

Back

Close

Full Screen / Esc

Printer-friendly Version

Interactive Discussion



## Abstract

This study uses aircraft measurements of relative humidity and ice crystal size distribution collected in synoptic cirrus during the SPARTICUS (Small PARTicles In Cirrus) field campaign to evaluate and constrain ice cloud parameterizations in the Community Atmosphere Model version 5. The probability density function (PDF) of ice crystal number concentration ( $N_i$ ) derived from high frequency (1 Hz) measurements features a strong dependence on ambient temperature. As temperature decreases from  $-35^\circ\text{C}$  to  $-62^\circ\text{C}$ , the peak in the PDF shifts from  $10\text{--}20\text{L}^{-1}$  to  $200\text{--}1000\text{L}^{-1}$ , while the ice crystal number concentration shows a factor of 6–7 increase.

Model simulations are performed with two different in-situ ice nucleation schemes. One of the schemes can reproduce a clear increase of  $N_i$  with decreasing temperature, by using either an observation based ice nuclei spectrum or a classical theory based spectrum with a relatively low (5–10%) maximum freezing ratio for dust aerosols. The simulation with the other scheme, which assumes a high maximum freezing ratio (100%), shows much weaker temperature dependence of  $N_i$ . Simulations are also performed to test empirical parameters related to water vapor deposition and the auto-conversion of ice crystals to snow. Results show that a value between 0.05 and 0.1 for the water vapor deposition coefficient and  $250\ \mu\text{m}$  for the critical ice crystal size can produce good agreements between model simulation and the SPARTICUS measurements in terms of ice crystal number concentration and effective radius. The climate impact of perturbing these parameters is also discussed.

## 1 Introduction

Microphysical processes in ice- and mixed-phase clouds have significant impacts on cloud radiative properties (Smith et al., 1998; Jensen et al., 2010) and precipitation formation (Heymsfield, 1977). Compared to the understanding of processes in warm clouds, our knowledge about ice particle formation and transformation are still very

## Evaluating ice cloud parameterizations in CAM5

K. Zhang et al.

Title Page

Abstract

Introduction

Conclusions

References

Tables

Figures

◀

▶

◀

▶

Back

Close

Full Screen / Esc

Printer-friendly Version

Interactive Discussion



limited (Kärcher and Spichtinger, 2009). In particular, details of the homogenous and heterogeneous nucleation processes under various atmospheric conditions, as well as their relative contributions to the formation of ice crystals in cold clouds, remain unclear (Sassen and Dodd, 1988; Detwiler, 1989; Jensen et al., 1998; DeMott et al., 2003; Cziczo et al., 2004; Prenni et al., 2007; Spichtinger and Gierens, 2009). The interactions among various cloud microphysical and macrophysical processes further complicate the situation, which results in large uncertainties in the parameterization of ice- and mixed-phase clouds in global climate models (GCM) (Mitchell et al., 2008; Kärcher and Burkhardt, 2008; Lohmann and Hoose, 2009; Gettelman et al., 2010; Salzmann et al., 2010; Wang and Penner, 2010; Yun and Penner, 2012).

There are a number of empirical parameters in ice parameterization schemes in current GCMs, and in cloud parcel models that are used to develop such parameterizations. For example, a parameter  $f_{\max}$  is commonly used in classical-theory-based heterogeneous ice nucleation schemes (e.g. Barahona and Nenes, 2009b; Hoose et al., 2010) to set an upper limit on the freezing fraction of the aerosol population. A larger  $f_{\max}$  can result in larger contribution from heterogeneous ice nucleation at warmer temperatures and potentially inhibit the homogeneous nucleation. For mineral dust particles (which are efficient ice nuclei), Liu et al. (2007) and Hoose et al. (2010) assumed the maximum ice-nucleating fraction (a concept very similar to  $f_{\max}$ ) to be 100% for immersion freezing, while Barahona and Nenes (2009b) used a  $f_{\max}$  value of 5%. Another example is the deposition coefficient  $\alpha$  (also called the mass accommodation coefficient) of water vapor which determines the diffusional growth efficiency of ice crystals. While Magee et al. (2006) inferred from laboratory measurements a most-likely range of 0.0045 to 0.0075 for ice particle growing at  $-50^{\circ}\text{C}$ , different values between 0.04 and 1 have been used in various models. Lin et al. (2002) pointed out that the total number of nucleated ice crystals simulated is very sensitive to the value of  $\alpha$  in seven parcel models. A similar finding was reported by Lohmann et al. (2008) using the ECHAM5 GCM. These sensitivities and discrepancies suggest that observational data are urgently needed to constrain empirical parameters in GCMs.

## Evaluating ice cloud parameterizations in CAM5

K. Zhang et al.

[Title Page](#)[Abstract](#)[Introduction](#)[Conclusions](#)[References](#)[Tables](#)[Figures](#)[◀](#)[▶](#)[◀](#)[▶](#)[Back](#)[Close](#)[Full Screen / Esc](#)[Printer-friendly Version](#)[Interactive Discussion](#)

## Evaluating ice cloud parameterizations in CAM5

K. Zhang et al.

Title Page

Abstract

Introduction

Conclusions

References

Tables

Figures

◀

▶

◀

▶

Back

Close

Full Screen / Esc

Printer-friendly Version

Interactive Discussion



There are currently two types of observational data available for ice crystal micro-physical properties: direct measurements (e.g. Krämer et al., 2009; Lawson, 2011), and remote-sensing data from satellites and/or ground-based instruments (e.g. Mace et al., 2005; Deng and Mace, 2006, 2008). For the purpose of quantitative comparison with model simulations, remote-sensing data need to be used with care because the quantities they provide strongly depend on the shapes and habits of ice particles assumed by the retrieval algorithms. These assumptions may not be consistent with those used in GCMs, thus can cause difficulties in interpreting the comparison results unless a proper simulator is used. In contrast, direct measurements are more straightforward to use and meanwhile have good data quality in general. Aircraft in situ observations are a good source of direct measurements, especially for high altitudes. The main limitation is the relatively small spatial and temporal coverage, with flights through cirrus clouds being even rarer. During the SPARTICUS (Small Particles In Cirrus) campaign (<http://acrf-campaign.arm.gov/sparticus/>), about 200 h of data were collected during a time span of six months. In addition, new two-dimensional stereo-imaging probes (2D-S) and improved algorithms designed by Lawson et al. (2006) and Lawson (2011) were employed to reduce possible biases in the measured ice crystal number concentration resulting from shattering of ice crystals on airborne instrument inlets. During the SPARTICUS campaign, ice crystal number concentration and size distribution as well as ambient meteorological variables were measured concurrently, providing valuable references for model development and evaluation.

In this work we use measurements from the SPARTICUS campaign to evaluate two ice cloud parameterization schemes in a global climate model and constrain three empirical parameters. We focus on the number concentration and size of ice crystals and their relationship with temperature, because the concentration and effective radius of condensates are the factors that determine the radiative properties of clouds and hence their impact on climate. Given that most of the measurements during SPARTICUS were collected in synoptic cirrus clouds, we concentrate on this cloud type in the present paper. This means we focus the analysis on in-situ ice nucleation in pure

ice-phase clouds, and do not touch the topic of droplet freezing in mixed-phase clouds. Discussion on detrainment of ice crystals from convective clouds is also excluded from this work because the number of flights with anvil occurrence is small in this campaign.

The remainder of the paper is organized as follows: Sect. 2 provides further details about the SPARTICUS aircraft measurements used in this study. Sections 3 and 4 summarize the ice cloud parameterization schemes in CAM5 and describe the simulations performed in this study. Results are shown and discussed in Sect. 5. Conclusions are drawn in Sect. 6.

## 2 SPARTICUS aircraft measurements

During the SPARTICUS field campaign, a SPEC Learjet aircraft collected about 200 h of in situ microphysics observations from January to June 2010 along trajectories between Boulder, CO and the ARM SGP site (Fig. 1). Number concentration and size distribution of ice crystals that have a maximum dimension  $D_{\max}$  between  $10\ \mu\text{m}$  and  $3000\ \mu\text{m}$  were measured by a 2D-S probe. The probe generates two orthogonal laser beams to create two-dimensional silhouettes of ice particles larger than  $10\ \mu\text{m}$ . Compared to conventional optical array probes (Knollenberg, 1970), the stereo view of particles in the laser-beam overlap region improves the sample volume boundaries and sizing of small ( $< 100\ \mu\text{m}$ ) particles. With improved probe tip design and particle inter-arrival time algorithms, the 2D-S probe can also reduce the shattering of ice particles and provide reliable ice crystal number measurements (Lawson, 2011). As small ice crystals ( $10\ \mu\text{m} < D_{\max} < 100\ \mu\text{m}$ ) dominate the ice particle population in cirrus cloud, the better measurement accuracy of 2D-S in this size range provides reliable data to evaluate the numerical model. Ambient temperatures were measured by the Rosemount probe (Model 102, precision:  $\pm 0.5^\circ\text{C}$ ). An open path Diode Laser Hygrometer (DLH) (precision:  $\pm 1\%$ ) was employed to measure the water vapor mixing ratio, which operates in the near-infrared spectral region ((Diskin et al., 2002)). In order to be consistent with the model calculation of relative humidity with respect to ice (RH<sub>i</sub>),

## Evaluating ice cloud parameterizations in CAM5

K. Zhang et al.

Title Page

Abstract

Introduction

Conclusions

References

Tables

Figures

◀

▶

◀

▶

Back

Close

Full Screen / Esc

Printer-friendly Version

Interactive Discussion



observation-derived RHi is calculated based on Goff and Gratch (1946) using water vapor mixing ratio, ambient pressure, and temperature. Effective diameter is derived from the observed ice crystal size distribution following Mitchell (2002). The observational data are available at the frequency of 1 Hz.

5 The aircraft trajectories covered various types of topography in this campaign, from the Rocky Mountains in the west to the relatively homogeneous geography over the Southern Great Plains (SGP) in the east (Fig. 1). In order to exclude possible biases in the model that are associated with the dynamical effects of complex topography, we do not use the whole data set from SPARTICUS but limit the model evaluation within  
10 a  $6^\circ \times 6^\circ$  (about  $600 \text{ km} \times 600 \text{ km}$ ) area centered at the SGP site (black square in Fig. 1). As our focus is on the role of in-situ ice nucleation in cirrus clouds, data from flights with anvil occurrence are also excluded. This leaves us more than 98 000 in-cirrus samples in total, with more than 10 thousand in each of the 10K temperature bins shown in Table 1. The large number of samples provide a solid basis for the statistical analysis  
15 of the ice crystal properties in Sect. 5.

### 3 Model

#### 3.1 CAM5 model

20 The GCM used in this study is the Community Atmosphere Model Version 5 (CAM5, Neale et al., 2010). The model uses finite volume methods in its dynamical core and tracer transport algorithm, with a standard horizontal resolution of  $1.9^\circ \times 2.5^\circ$  (latitude by longitude) and a time step of 30 min. Large-scale condensation, cloud fraction calculation, and the horizontal and vertical overlapping of clouds are handled by a cloud macrophysics parameterization of Park et al. (2012). Stratiform microphysical processes are represented by a two-moment scheme that solves prognostic equations  
25 for cloud droplet and cloud ice, and diagnostic equations for rain and snow (Morrison and Gettelman, 2008; Gettelman et al., 2008). As atmospheric aerosols play a key role

## Evaluating ice cloud parameterizations in CAM5

K. Zhang et al.

Title Page

Abstract

Introduction

Conclusions

References

Tables

Figures

◀

▶

◀

▶

Back

Close

Full Screen / Esc

Printer-friendly Version

Interactive Discussion



in supplying cloud condensation nuclei and ice nuclei (IN), a modal aerosol module (MAM) (Liu et al., 2012a) is incorporated to interactively predict mass and number concentrations of various aerosol species. Moist turbulence and shallow convection are parameterized by the schemes of Bretherton and Park (2009) and Park and Bretherton (2009), respectively. Deep convection is treated with the parameterization of Zhang and McFarlane (1995) with further modifications by Richter and Rasch (2008). Short-wave and longwave radiative transfer calculations are performed using the RRTMG code (Iacono et al., 2008; Mlawer et al., 1997). Details of the model formulation are described by Neale et al. (2010).

### 3.2 Ice nucleation

The formation of ice crystals in stratiform clouds considered in CAM5 includes in-situ ice nucleation in cirrus clouds, in-situ droplet freezing in mixed-phase clouds, and detrainment of ice crystals from convective clouds formed by either shallow or deep convection. Table 2 summarizes the ambient conditions under which these mechanisms can take effect. In this study we focus on the in-situ ice nucleation in cirrus clouds.

The ice nucleation scheme used in CAM5 originated from the parameterization of Liu et al. (2007). It was derived as an empirical fit of a parcel model simulation performed by Liu and Penner (2005, hereafter LP05) in which the nucleation rates were calculated with the classical nucleation theory. Based on Liu et al. (2007), Gettelman et al. (2010) coupled LP05 with Morrison and Gettelman (2008) cloud microphysics and the aerosol module MAM. It has also adopted the cloud macrophysics closure proposed by Park et al. (2012), and allows supersaturation with respect to ice. Despite these changes, the in-situ ice nucleation stays the same as in Liu et al. (2007), i.e. the empirical fit of results from LP05. It is worth noting that the parcel model simulation in LP05 was performed with a set of prescribed parameters (e.g. the water vapor deposition coefficient). The empirical fit was implemented in the CAM5 model as a look-up table. If one intended to carry out CAM5 simulations with different values for these parameters, it would be

## Evaluating ice cloud parameterizations in CAM5

K. Zhang et al.

Title Page

Abstract

Introduction

Conclusions

References

Tables

Figures



Back

Close

Full Screen / Esc

Printer-friendly Version

Interactive Discussion



necessary to re-run the parcel model and re-derive the look-up table. This severely limits the flexibility of the LP05 ice nucleation parameterization.

Recently Liu et al. (2012b) implemented in CAM5 a physically based parameterization for the in-situ ice nucleation in cirrus clouds, originally proposed by Barahona and Nenes (2008) and later extended by Barahona and Nenes (2009a,b, hereafter BN09). The BN09 parameterization explicitly considers effects of water vapor deposition on simulated ice crystals number concentration. It also provides the flexibility of using different IN spectra (with respect to ambient conditions) for the heterogeneous nucleation calculation. The default configuration uses an empirical spectrum derived from observation (Phillips et al., 2008). Optionally, one can choose to use spectra derived from classical nucleation theory (Barahona and Nenes, 2009b). Furthermore, the scheme can be extended to consider the effect of pre-existing ice crystals on ice nucleation (Barahona, 2012, personal communication). The BN09 scheme provides a flexible basis for investigating the uncertainties associated with empirical parameters.

For cirrus clouds, both the LP05 and BN09 schemes include homogeneous nucleation on sulfate, heterogeneous immersion freezing on mineral dust, as well as competition between the two mechanisms. The number concentration of nucleated ice crystals is computed as a function of temperature, humidity, aerosol (sulfate and dust) number concentration, and sub-grid updraft velocity. The sub-grid updraft velocity is derived from the turbulent kinetic energy (TKE) calculated by the moist turbulence scheme of Bretherton and Park (2009), with an assumed maximum value of  $0.2 \text{ ms}^{-1}$  (Gettelman et al., 2010).

In addition to in-situ ice nucleation in cirrus, cloud droplets can freeze to form ice crystals too. Deposition/condensation freezing is considered in the model based on Meyers et al. (1992), with a constant freezing rate. Contact freezing of cloud droplets is included based on Young (1974) using the number concentration of coarse mode dust. Homogeneous freezing of cloud droplets is assumed to occur instantaneously at  $-40^\circ\text{C}$ . Ice crystals detrained from the convective clouds are distributed into the

## Evaluating ice cloud parameterizations in CAM5

K. Zhang et al.

Title Page

Abstract

Introduction

Conclusions

References

Tables

Figures

◀

▶

◀

▶

Back

Close

Full Screen / Esc

Printer-friendly Version

Interactive Discussion



environment by assuming a mean volume radius of 50  $\mu\text{m}$  for shallow convection and 25  $\mu\text{m}$  for deep convection. More details can be found in Table 2 and references therein.

## 4 Experimental design

CAM5 simulations presented in this paper are summarized by Table 3. The horizontal and vertical resolutions are  $1.9^\circ \times 2.5^\circ$  (latitude  $\times$  longitude) and 30 vertical levels, respectively. The model time step is 30 min. For each simulation, we run the model for 5 yr plus 3 months of spin-up, driven by climatological sea surface temperatures and sea ice extent. Emissions of aerosols and their precursors are prescribed according to Lamarque et al. (2010) using the year 2000 set-up.

In order to compare model results with the SPARTICUS measurements, 3-hourly instantaneous output are obtained over the SGP area. Instantaneous values are used to calculate probability density functions (PDFs) of the number concentration and effective diameter of ice crystals as well as their relationship with temperature. For the purpose of (i) identifying the dominant mechanisms of in-situ ice nucleation and (ii) following the same sampling conditions as in observation, we also included in model output the tendency rates related to processes listed in Table 2.

In total we have carried out 15 simulations in 4 groups. Group A first compares the behavior of the LP05 and BN09 schemes in their default configuration that includes the competition between homogeneous and heterogeneous nucleation (simulations LP and BN). To help understand the relative contributions of different nucleation mechanisms, two additional sensitivity tests are performed with each parameterization, with only homogeneous (LPHOM and BNHOM) or heterogeneous (LPHET and BNHET) nucleation switched on in cirrus clouds. The representation of mixed-phase clouds is kept the same.

In the other three groups of simulations (B, C and D) we use the BN09 scheme to investigate the sensitivity of ice cloud simulations to empirical parameters. Selected values based on literature review are applied, and their effects evaluated by contrasting

## Evaluating ice cloud parameterizations in CAM5

K. Zhang et al.

Title Page

Abstract

Introduction

Conclusions

References

Tables

Figures

◀

▶

◀

▶

Back

Close

Full Screen / Esc

Printer-friendly Version

Interactive Discussion



the results and comparing them with observations. Further details of the parameters and the values used in our simulations are given below.

Simulations in Group B replaces the empirical IN spectrum for heterogeneous ice nucleation in the default BN09 scheme by a classical theory based spectrum of Barahona and Nenes (2009b). In this configuration, a prescribed parameter  $f_{\max}$  (the maximum freezing fraction of the aerosol population) limits the number of ice nuclei, thus has a direct impact on heterogeneous ice nucleation. In numerical models, the  $f_{\max}$  of each aerosol type is usually prescribed according to the observed typical maximum values (Möhler et al., 2006; Field et al., 2006; Phillips et al., 2008). For mineral dust, both Hoose et al. (2010) and LP05 assumed the maximum ice-nucleating fraction to be 100 % for immersion freezing, while the BN09 parameterization uses the value 5 %. In simulation Group B, three additional values (10 %, 50 % and 100 %) are tested.

Simulations in Group C investigate the impact of the water vapor deposition coefficient  $\alpha$ . Earlier studies (e.g. Lin et al., 2002; Comstock et al., 2008; Lohmann et al., 2008) have shown that the model-predicted ice crystal number concentration can be very sensitive to this coefficient. This is because ice nucleation and crystal growth compete for the available water vapor in the atmosphere. A smaller (larger) deposition coefficient will lead to a longer (shorter) period during which the relative humidity stays near the critical value for nucleation, and consequently higher (lower) concentrations of the nucleated ice crystals (Gierens, 2003). The values of this parameter derived from earlier laboratory experiments and field measurements range from about 0.01 to 1.0 (cf. Table 5.5 of Pruppacher and Klett, 1997, and Lin et al., 2002). Magee et al. (2006) found in laboratory measurements that the most-likely value for representative particle growing at  $-50^{\circ}\text{C}$  is between 0.0045 and 0.0075. A parcel modeling study by Kay and Wood (2008) suggests that the deposition coefficient varies with ice crystal size and magnitude of supersaturation. These results indicate that an accurate value of  $\alpha$  has not yet been established. The default parameter in the BN09 parameterization is  $\alpha = 0.1$ , while other models and schemes used various values between 0.04 and 1 (cf.

## Evaluating ice cloud parameterizations in CAM5

K. Zhang et al.

Title Page

Abstract

Introduction

Conclusions

References

Tables

Figures

◀

▶

◀

▶

Back

Close

Full Screen / Esc

Printer-friendly Version

Interactive Discussion



Table 4). In simulation Group C, we test three values ( $\alpha = 0.006, 0.05, 0.5$ ) that span two orders of magnitude, and compare the results with the reference BN simulation.

In the bulk cloud microphysical schemes of Morrison and Gettelman (2008), a critical particle diameter  $D_{cs}$  is defined to distinguish cloud ice and snow as two different classes of solid-phase condensates. The so-called autoconversion rate, i.e. the rate at which ice crystals are converted into snow, is calculated in CAM5 by integrating the cloud ice size distribution over the range  $[D_{cs}, \infty)$  and transferring the resulting condensate to the snow category (Ferrier, 1994; Morrison and Gettelman, 2008). Gettelman et al. (2010) found that the separating size  $D_{cs}$  has a strong impact on the simulated ice water path and total cloud forcing. Various  $D_{cs}$  values have been used in recent versions of the CAM5 model (cf. Table 5) to achieve the top-of-atmosphere radiative balance in long-term climate simulations, although such tuning may cause biases in the simulated microphysical processes and ice crystal size in the atmosphere. In Group D of our simulations, four different values of  $D_{cs}$  (400  $\mu\text{m}$ , 325  $\mu\text{m}$ , 250  $\mu\text{m}$  and 175  $\mu\text{m}$ ) are evaluated.

## 5 Results

### 5.1 LP05 versus BN09 scheme

The overall performance of the LP05 and BN09 schemes in CAM5 in global climate simulation has been evaluated by Gettelman et al. (2010) and Liu et al. (2012b). The analysis here takes a different perspective and focuses on synoptic cirrus.

The ice crystal number concentrations ( $N_i$ ) in the SGP area measured during the SPARTICUS campaign and simulated with the LP05 and BN09 in-situ ice nucleation schemes are presented in Fig. 2 for four temperature ranges. The numbers given here are in-cirrus values in the upper troposphere (above 500 hPa). In the observational data, both the mean and median concentrations feature a marked increase with decreasing temperature (Fig. 2a). Consistently, the PDF of  $N_i$  shown in Fig. 3a features

## Evaluating ice cloud parameterizations in CAM5

K. Zhang et al.

Title Page

Abstract

Introduction

Conclusions

References

Tables

Figures

◀

▶

◀

▶

Back

Close

Full Screen / Esc

Printer-friendly Version

Interactive Discussion



a clear shift of the peak from  $10\text{--}20\text{ L}^{-1}$  at  $-35^\circ\text{C}$  to  $200\text{--}1000\text{ L}^{-1}$  at temperatures below  $-60^\circ\text{C}$ . The BN09 scheme can reproduce an increase of the mean  $N_i$  with decreasing temperature (Fig. 2b), although not as strong as in the observation, while the LP09 scheme gives rather constant  $N_i$  values (Fig. 2c). For both schemes, the homogenous-only simulations feature a shift of the  $N_i$  PDF towards higher concentrations at lower temperature, while the heterogeneous-only simulations does not show this trend (Fig. 3). The temperature dependence of  $N_i$  PDF in the default BN simulation (Fig. 3b) looks very similar to BNHOM (homogenous-only, Fig. 3c). The default LP run (Fig. 3e), in contrast, appears more similar to the corresponding heterogeneous-only simulation (Fig. 3g). This suggests that the relative contributions of the two nucleation mechanisms are different in LP and BN.

To provide more quantitative evidence for this statement, the left panel in Fig. 4 shows a breakdown of the ice crystal number production rate (i.e. the number of newly produced ice crystals per liter per model time step) at 200 hPa in the default LP and BN simulations. While homogeneous and heterogeneous nucleation play similar roles in crystal number production in LP, the BN simulation is dominated by homogenous nucleation. In the right panel of the same figure, the nucleation frequency – defined as the number of occurrence of (homogeneous or heterogeneous) nucleation event divided by the total number of model time steps – is compared between the two schemes. (The two mechanisms can be active at the same time.) The chart shows similar heterogeneous nucleation frequencies in the two simulations, but a factor-of-10 difference in the homogeneous nucleation frequency. The same analyses have been repeated for other pressure levels in the upper troposphere and led to similar results (not shown). Figure 4 thus confirms that the ice crystal number concentrations simulated using the default BN scheme is dominated by homogenous nucleation, while the heterogeneous nucleation plays a much more important role in the LP simulation. Furthermore, we note that this difference is not only seen in the SGP area but also generally present in most other regions around the globe, as can be seen in Fig. 5 where the zonally and annually averaged in-cloud  $N_i$  are shown for all simulations in Group A. The BN09 simulations

## Evaluating ice cloud parameterizations in CAM5

K. Zhang et al.

[Title Page](#)[Abstract](#)[Introduction](#)[Conclusions](#)[References](#)[Tables](#)[Figures](#)[◀](#)[▶](#)[◀](#)[▶](#)[Back](#)[Close](#)[Full Screen / Esc](#)[Printer-friendly Version](#)[Interactive Discussion](#)

with and without heterogeneous nucleation give rather similar results (panel b), while the homogenous-only LP05 simulation features considerably higher  $N_i$  than the default configuration (panel a).

In the model, sufficiently high relative humidity with respect to ice ( $RH_i$ ) is one of the key conditions for ice nucleation to occur (cf. Table 2). To check whether this is the cause of the differences between the LP and BN simulations, Fig. 6 compares the simulated and observed bivariate PDF of  $RH_i$  and ambient temperature in different cases distinguished by the ice crystal number concentration. The clear-sky cases (Fig. 6, left column) are also included here to take into account the initial stage of cirrus formation. Following Haag et al. (2003),  $RH_i$  values higher than water saturation are not included in the analysis. In CAM5,  $RH_i$  diagnosed in different parts of the time integration procedure can have different values due to the time splitting algorithm. The values we present here are those used in the ice nucleation calculation.

The SPARTICUS data clearly reveals lower  $RH_i$  in clear sky than inside cirrus (Fig. 6a versus b), although high ice-supersaturation ( $> 120\%$ ) can happen in both cases. Such high ice-supersaturation over the SGP area has already been reported before (Comstock et al., 2004). Both inside and outside cirrus, higher  $RH_i$  values are observed at lower temperatures. This is in agreement with earlier studies by Ovarlez et al. (2002) and Spichtinger et al. (2004), where it was shown that the shape of the in-cloud humidity PDF changes from nearly symmetric about ice saturation in relatively warm cirrus to considerably positively skewed in colder clouds. Inside cirrus clouds, cases with higher crystal number concentration (Fig. 6d) are more often associated with lower temperature and higher humidity (e.g.  $T \leq -50^\circ\text{C}$ ,  $RH_i \geq 130\%$ ) than the cases with lower  $N_i$  (Fig. 6c).

In a qualitative sense, these features are captured by the model to some extent, despite a general underestimate of supersaturation (Fig. 6 second and third rows). In the model, the air is ice-supersaturated about 33 % of the time inside cirrus clouds, significant lower than the observed percentage (56 %) during SPARTICUS. Below  $-45^\circ\text{C}$ , the simulated peaks of the in-cloud  $RH_i$  PDF appear persistently around ice-saturation,

## Evaluating ice cloud parameterizations in CAM5

K. Zhang et al.

Title Page

Abstract

Introduction

Conclusions

References

Tables

Figures

◀

▶

◀

▶

Back

Close

Full Screen / Esc

Printer-friendly Version

Interactive Discussion



rather than shift towards higher values as temperature decreases. These biases are not unexpected given the rather coarse resolution of global climate models as well as the lack of explicit representation of sub-grid variability (cf. e.g. Kärcher and Burkhardt, 2008; Wang and Penner, 2010). As a primitive remedy, CAM5 assumes the threshold supersaturation for ice nucleation in a grid box is reached at a value 20 % lower than the real threshold (Neale et al., 2010; Liu et al., 2012b).

Regardless of the discrepancies between observation and model simulation, we can see from Fig. 6 that the relative humidity in the LP and BN simulations are very similar. Therefore the  $RH_i$  can not explain the different ice nucleation frequencies in the two simulations. We have also checked other conditions that directly affect ice nucleation in the model, e.g. sub-grid updraft velocity and number concentration of sulfate and dust particles. They appear to be also rather similar between the two simulations.

## 5.2 Sensitivity to $f_{\max}$

In the previous subsection, the LP and BN simulations are performed with the default configuration of the corresponding ice nucleation scheme, i.e. using a classical-nucleation-theory (CNT) based IN spectrum for heterogeneous nucleation in LP and an observation based empirical spectrum in BN. In order to find the reason for the different results from the LP and BN simulations in Group A, we start Group B with experiment BNCNT in which the CNT-based IN spectra of Barahona and Nenes (2009b) is used. In addition, the spectrum is adjusted by applying different values for the maximum freezing ratio of potential ice nuclei ( $f_{\max}$ ).

The  $N_i$  PDFs in the SGP region given by this set of simulations are shown in Fig. 7. As  $f_{\max}$  increases from 5 % to 100 % (panels a to d), the peak of the PDF in the low-temperature range ( $< -55^\circ\text{C}$ ) gradually shifts to lower concentrations. For the two simulations with the largest and smallest  $f_{\max}$ , we calculated the breakdown of ice crystal production and the nucleation frequencies as in the previous section. While the BNCNT run with  $f_{\max} = 5\%$  produces similar results to the default BN simulation in Group A, the BNCNT run with  $f_{\max} = 100\%$  turns out remarkably similar to the LP simulation

## Evaluating ice cloud parameterizations in CAM5

K. Zhang et al.

Title Page

Abstract

Introduction

Conclusions

References

Tables

Figures

◀

▶

◀

▶

Back

Close

Full Screen / Esc

Printer-friendly Version

Interactive Discussion



(Fig. 8). With a larger  $f_{\max}$  (i.e. more IN), not only are more crystals produced by heterogeneous nucleation (Fig. 8, left panel), but also the homogeneous nucleation becomes suppressed (Fig. 8, right panel) and contributes considerably less to the total crystal production (Fig. 8, left panel). Consequently the total  $N_i$  in the SGP region decreases by more than 60 % (not shown). As for the global scale, Fig. 9 illustrates the annually and zonally averaged ice crystal number concentration in the two simulations. In the Northern Hemisphere where the main sources of dust aerosols are located, a larger  $f_{\max}$  leads to considerably less ice crystals between 100 and 200 hPa. (In Fig. 9c, differences that are insignificant in comparison to the natural variability have been masked out.)

Results from this set of sensitivity experiments indicate that differences in the IN spectrum are probably the main reason for the discrepancies seen earlier between the default LP and BN simulations. Better agreement with the SPARTICUS measurements can be obtained either with an observation-based spectrum, or a CNT-based spectrum with a rather low freezing ratio (5 %). A larger  $f_{\max}$  (as, e.g. in the LP05 scheme) causes stronger heterogeneous nucleation and suppressed homogeneous nucleation, which can result in lower ice crystal number concentration in global simulations.

### 5.3 Sensitivity to the water vapor deposition coefficient $\alpha$

In the BN09 ice nucleation scheme, the water vapor deposition coefficient  $\alpha$  is a tunable parameter that directly affects the supersaturation over ice (cf. Eqs. 1 and 4–6 in Barahona and Nenes, 2008) which then determines the size distribution of ice crystals. This reflects the competition for available water vapor between crystal formation and crystal growth. Simulations in Group C reveal that an increase of  $\alpha$  from the default value 0.1 to 0.5 leads to little change in the results (Fig. 10a), while a decrease in the parameter results in shifts of the  $N_i$  PDF at all temperatures shown in Fig. 10. In the SGP region,  $\alpha = 0.05$  gives the best agreement between simulated and the measured  $N_i$ , while the value 0.006, based on laboratory measurements at  $-50^\circ\text{C}$  from Magee et al. (2006), leads to about 400 % positive biases at this and lower temperatures (not

## Evaluating ice cloud parameterizations in CAM5

K. Zhang et al.

[Title Page](#)[Abstract](#)[Introduction](#)[Conclusions](#)[References](#)[Tables](#)[Figures](#)[◀](#)[▶](#)[◀](#)[▶](#)[Back](#)[Close](#)[Full Screen / Esc](#)[Printer-friendly Version](#)[Interactive Discussion](#)

shown). Compared to the default configuration ( $\alpha = 0.1$ ), the crystal number concentrations simulated with  $\alpha = 0.006$  are about factor of 9 higher at and below  $-50^\circ\text{C}$ , similar to results obtained by Lohmann et al. (2008) with the ECHAM5 model.

On the global scale, decreasing  $\alpha$  from 0.1 to 0.05 and 0.006 can lead to more than 50 % ( $\alpha = 0.05$ ) and a factor of 5 ( $\alpha = 0.006$ ) increases of  $N_i$ , respectively in the upper troposphere (excluding tropical regions, Fig. 11). Unlike  $f_{\text{max}}$  which mainly affects the Northern Hemisphere middle and high latitudes, the impact of  $\alpha$  is global, and more symmetric with respect to the equator.

#### 5.4 Sensitivity to the critical crystal diameter $D_{\text{cs}}$

The critical diameter  $D_{\text{cs}}$  that separates cloud and snow is an artificial parameter in bulk cloud microphysics parameterizations. In the scheme of Morrison and Gettelman (2008), it shows up only in the autoconversion from ice crystal to snow. With a larger  $D_{\text{cs}}$ , less crystals are converted to the snow class and precipitate, resulting in a larger average size of the ice crystals remaining in the atmosphere. This is indeed seen in the crystal effective diameter at all temperature ranges shown in Fig. 12 (orange-colored triangles). The  $D_{\text{cs}}$  value of  $250\ \mu\text{m}$  produces a simulation that matches best with the SPARTICUS measurements. The algorithm used for deriving the observed effective diameter is described by Mitchell et al. (2011).  $D_{\text{cs}} = 350\ \mu\text{m}$  and  $400\ \mu\text{m}$  (the default values in CAM5.0 and CAM5.1, respectively) result in larger effective diameters for ice crystals (Fig. 12c, d) and little change in crystal number concentration (not shown). Consequently the ice water path is larger, and so is the longwave cloud forcing (Table 6).

It is worth noting that the measurements from SPARTICUS may contain snow particles of up to  $3000\ \mu\text{m}$  due to the characteristics of the instruments. The observation-based effective diameters in Fig. 12 thus may contain positive biases especially at warmer temperatures. Based on this consideration, the overestimated effective diameters in the model with  $D_{\text{cs}} = 350\ \mu\text{m}$  and  $400\ \mu\text{m}$  suggest that these values for the separating diameter are indeed on the large side. Although the top-of-atmosphere radiative

## Evaluating ice cloud parameterizations in CAM5

K. Zhang et al.

Title Page

Abstract

Introduction

Conclusions

References

Tables

Figures



Back

Close

Full Screen / Esc

Printer-friendly Version

Interactive Discussion



balance is achieved in the corresponding model versions, the partition of radiative forcing between cold and warm clouds may be biased.

## 5.5 Climate impact

Results presented above indicate that the simulated ice crystal size and number concentration are sensitive to empirical parameters in cloud microphysics including ice nucleation parameterization. To assess the climate impact, Table 6 lists key variables that describe the global mean cloud forcing and hydrological cycle in the sensitivity simulations.

Among the four groups of simulations, the selected metrics are most sensitive to the water vapor deposition coefficient  $\alpha$  and the crystal/snow separating diameter  $D_{cs}$ . When the deposition coefficient is changed from 0.1 to 0.006, the more than factor-of-5 higher  $N_i$  in the upper troposphere (Fig. 11b) results in a LWCF increase of about  $15 \text{ W m}^{-2}$ , a high-cloud fraction increase of about 20 %, and an ice water path (IWP) increase of 30 %. The surface precipitation rate reduces by about 11 %. The simulated LWCF ( $47.1 \text{ W m}^{-2}$ ) becomes too far away from the observation ( $27 \text{ W m}^{-2}$ ). With  $\alpha = 0.05$ , the LWCF, high-cloud fraction, and ice water path are also larger than those simulated with the default value, but the changes are moderate.

The critical diameter  $D_{cs}$  also has clear impacts on the simulated climate, explaining why it is often used as the main tuning parameter for radiative balance. When the value is changed from  $400 \mu\text{m}$  to  $250 \mu\text{m}$  which matches the observation, the simulated IWP decreases by 37 % and the longwave cloud forcing decreases by  $1 \text{ W m}^{-2}$ . The ice crystal number is only slightly higher because of weaker sedimentation sink (not shown). Because the IWP is smaller, the Bergeron-Findeisen process is less sufficient and the liquid water path (LWP) becomes larger. The shortwave cloud forcing increases by  $1.9 \text{ W m}^{-2}$  primarily due to the larger LWP.

$f_{\text{max}}$  has a relatively small impact on the global mean metrics because it is directly related to the heterogeneous nucleation thus the influence is limited in terms of spatial coverage.

## Evaluating ice cloud parameterizations in CAM5

K. Zhang et al.

Title Page

Abstract

Introduction

Conclusions

References

Tables

Figures

◀

▶

◀

▶

Back

Close

Full Screen / Esc

Printer-friendly Version

Interactive Discussion



## 6 Conclusions

In this work, we used aircraft measurements of ice crystal size distribution and relative humidity collected during the SPARTICUS campaign to evaluate and constrain ice cloud parameterizations in CAM5. The measurements from synoptic cirrus clouds reveal a strong dependency of  $N_i$  on ambient temperature. As temperature decreases from  $-35^\circ\text{C}$  (about 240 K) to  $-62^\circ\text{C}$  (about 210 K), the peak in the  $N_i$  PDF shifts from  $10\text{--}20\text{ L}^{-1}$  to  $200\text{--}1000\text{ L}^{-1}$ . Consistently, the observed  $N_i$  shows a factor of 6–7 increase. These features appear different from the observational data used in Fig. 5 of Liu et al. (2012b), where measurements obtained by Krämer et al. (2009) from different regions (tropics, mid-latitudes, Arctic) and different types of cirrus (anvil, synoptic) were compiled together for model evaluation. The differences suggest that zooming into a specific (Northern Hemisphere mid-latitude) region and a particular type of cirrus clouds can provide more detailed information to support quantitative evaluation of process-based models and parameterizations.

Our results show that the above-mentioned temperature dependency of  $N_i$  in the SGP area can be reproduced by the CAM5 model when using the BN09 ice nucleation parameterization but not with the LP05 scheme, due to differences in the relative contribution of different nucleation mechanisms. Sensitivity simulations in Groups A and B further identify the IN spectrum as the key reason. When a classical-theory-based IN spectrum is used in combination with a high maximum freezing ratio  $f_{\text{max}}$  of the aerosol population (as in the LP05 scheme and in the BNCNT\_F100 simulation), the heterogeneous nucleation plays an important role in ice crystal production, and strongly suppresses the homogeneous nucleation. In contrast, when  $f_{\text{max}}$  is set to 5% or when an observation-based empirical IN spectrum is used, homogeneous nucleation plays a dominant role in ice crystal production, and the increase of  $N_i$  at colder temperature can be better reproduced. At the global scale, the impact can be clearly seen in the Northern Hemisphere where the main sources of dust aerosol are located. These re-

### Evaluating ice cloud parameterizations in CAM5

K. Zhang et al.

[Title Page](#)[Abstract](#)[Introduction](#)[Conclusions](#)[References](#)[Tables](#)[Figures](#)[◀](#)[▶](#)[◀](#)[▶](#)[Back](#)[Close](#)[Full Screen / Esc](#)[Printer-friendly Version](#)[Interactive Discussion](#)

sults suggest that using high  $f_{\max}$  for classical-theory-based IN spectrum may lead to overestimate of the climate impact of dust aerosols on cirrus clouds.

5 Simulations in Group C tested the sensitivity to the water vapor deposition coefficient  $\alpha$  used in the homogeneous nucleation of BN09. Within the tested range (0.5–0.006), a smaller  $\alpha$  leads to higher crystal number concentrations on the global scale, larger ice water path, and stronger longwave and shortwave cloud forcing. The value 0.05 gives the best fit of the simulated  $N_i$  in the SGP area, while the value 0.006 (based on laboratory experiments at  $-50^\circ\text{C}$ ) leads to overly high crystal concentrations at all temperature ranges investigated in this study, and too strong cloud radiative forcing.  
10 We therefore recommend a value between 0.05 and 0.1 for the CAM5 model.

The critical crystal diameter  $D_{\text{cs}}$  that distinguishes cloud ice and snow as two different classes of solid-phase condensates in the Morrison and Gettelman (2008) cloud microphysics parameterization has been used as a main tuning parameter in recent model versions to achieve the top-of-atmosphere radiative balance in the CAM5 model. While  
15 our comparison indicates  $D_{\text{cs}} = 250\ \mu\text{m}$  to provides the best agreement with the SPARTICUS campaign, the default values used in CAM5.0 ( $325\ \mu\text{m}$ ) and CAM5.1 ( $400\ \mu\text{m}$ ) result in positive biases in the ice crystal effective diameter. This suggest that in the model, the global mean radiative balance has been achieved at the expense of biases in the microphysical properties of ice crystals, and possibly also in the relative contribution of the radiative forcing from cirrus clouds.  
20

In the future, it will be useful to extend our analyses to more geographical domains and other cold cloud types, when new measurements become available. Assimilation techniques such as nudging can provide model capabilities that further facilitate comparison with observations. Moreover, there are many other empirical parameters in  
25 the model that are not yet well constrained. In our BN simulation, although the crystal number concentrations at low temperatures are better simulated than with the LP05 scheme, they are still significantly underestimated in comparison to the SPARTICUS measurements. One possible reason is the negative biases in the sub-grid updraft velocity used by the ice nucleation scheme, because lower updraft velocity may affect

## Evaluating ice cloud parameterizations in CAM5

K. Zhang et al.

[Title Page](#)[Abstract](#)[Introduction](#)[Conclusions](#)[References](#)[Tables](#)[Figures](#)[◀](#)[▶](#)[◀](#)[▶](#)[Back](#)[Close](#)[Full Screen / Esc](#)[Printer-friendly Version](#)[Interactive Discussion](#)

the competition between homogeneous and heterogeneous ice nucleation and lead to less frequent homogeneous nucleation (cf. DeMott et al., 1997; Jensen et al., 1994; Kärcher and Lohmann, 2003; Gettelman et al., 2012). We are currently investigating this issue and will report the results in a separate paper.

5 *Acknowledgements.* We thank Paul Lawson (SPEC Inc.) for his help with the ice crystal number concentration measured by the 2D-S probe and Glenn S. Diskin (NASA Langley Research Center) for the DLH water vapor measurements. We are also grateful to Xiangjun Shi (IAP/CAS), Eric Jensen (NASA Ames), Donifan Barahona (NASA GSFC), Hugh Morrison (NCAR), and Phil Rasch for helpful discussions. Comments and suggestions from Hui Wan provided through  
10 the PNNL internal review are highly appreciated. Kai Zhang and Xiaohong Liu acknowledge support from the NASA Modeling, Analysis and Prediction (MAP) Program. Xiaohong Liu and Minghuai Wang acknowledge support from the DOE Atmospheric System Research (ASR) Program. Jennifer M. Comstock was supported by the DOE Atmospheric Radiation Measurement (ARM) program. The Pacific Northwest National Laboratory is operated for DOE by Battelle  
15 Memorial Institute under contract DE-AC06-76RLO 1830.

## References

- Barahona, D. and Nenes, A.: Parameterization of cirrus cloud formation in large-scale models: homogeneous nucleation, *J. Geophys. Res.*, 113, D11, doi:10.1029/2007JD009355, 2008. 1208, 1215, 1230, 1232
- 20 Barahona, D. and Nenes, A.: Parameterizing the competition between homogeneous and heterogeneous freezing in cirrus cloud formation – monodisperse ice nuclei, *Atmos. Chem. Phys.*, 9, 369–381, doi:10.5194/acp-9-369-2009, 2009a. 1208
- Barahona, D. and Nenes, A.: Parameterizing the competition between homogeneous and heterogeneous freezing in ice cloud formation – polydisperse ice nuclei, *Atmos. Chem. Phys.*,  
25 9, 5933–5948, doi:10.5194/acp-9-5933-2009, 2009b. 1203, 1208, 1210, 1214, 1230, 1231
- Bretherton, C. S. and Park, S.: A new moist turbulence parameterization in the Community Atmosphere Model, *J. Climate*, 22, 3422–3448, doi:10.1175/2008JCLI2556.1, 2009. 1207, 1208

## Evaluating ice cloud parameterizations in CAM5

K. Zhang et al.

Title Page

Abstract

Introduction

Conclusions

References

Tables

Figures

◀

▶

◀

▶

Back

Close

Full Screen / Esc

Printer-friendly Version

Interactive Discussion



## Evaluating ice cloud parameterizations in CAM5

K. Zhang et al.

Title Page

Abstract

Introduction

Conclusions

References

Tables

Figures

◀

▶

◀

▶

Back

Close

Full Screen / Esc

Printer-friendly Version

Interactive Discussion



Comstock, J. M., Ackerman, T., and Turner, D.: Evidence of high ice supersaturation in cirrus clouds using ARM Raman lidar measurements, *Geophys. Res. Lett.*, 31, L11106, doi:10.1029/2004GL019705, 2004. 1213

Comstock, J. M., Lin, R.-F., Starr, D., and Yang, P.: Understanding ice supersaturation, particle growth, and number concentration in cirrus clouds, *J. Geophys. Res.*, 113, D23211, doi:10.1029/2008JD010332, 2008. 1210

Cziczo, D. J., Murphy, D. M., Hudson, P. K., and Thomson, D. S.: Single particle measurements of the chemical composition of cirrus ice residue during CRYSTAL-FACE, *J. Geophys. Res.-Atmos.*, 109, 4201, doi:10.1029/2003JD004032, 2004. 1203

DeMott, P., Meyers, M., and Cotton, W.: Parameterization and impact of ice initiation processes relevant to numerical model simulations of cirrus clouds, *J. Atmos. Sci.*, 51, 77–90, doi:10.1175/1520-0469(1994)051<0077:PAIOII>2.0.CO;2, 1994. 1232

DeMott, P., Rogers, D., and Kreidenweis, S.: The susceptibility of ice formation in upper tropospheric clouds to insoluble aerosol components, *J. Geophys. Res.*, 102, 19575–19584, doi:10.1029/97JD01138, 1997. 1220

DeMott, P. J., Rogers, D. C., Kreidenweis, S. M., Chen, Y., Twohy, C. H., Baumgardner, D., Heymsfield, A. J., and Chan, K. R.: The role of heterogeneous freezing nucleation in upper tropospheric clouds: inferences from SUCCESS, *Geophys. Res. Lett.*, 25, 1387–1390, doi:10.1029/97GL03779, 1998. 1232

DeMott, P. J., Cziczo, D. J., Prenni, A. J., Murphy, D. M., Kreidenweis, S. M., Thomson, D. S., Borys, R., and Rogers, D. C.: Measurements of the concentration and composition of nuclei for cirrus formation, *P. Natl. Acad. Sci. USA*, 100, 14655–14660, doi:10.1073/pnas.2532677100, 2003. 1203

Deng, M. and Mace, G. G.: Cirrus microphysical properties and air motion statistics using cloud radar Doppler moments. Part I: Algorithm description, *J. Appl. Meteorol. Climatol.*, 45, 1690, doi:10.1175/JAM2433.1, 2006. 1204

Deng, M. and Mace, G. G.: Cirrus microphysical properties and air motion statistics using cloud radar Doppler moments. Part II: Climatology, *J. Appl. Meteorol. Climatol.*, 47, 3221, doi:10.1175/2008JAMC1949.1, 2008. 1204

Detwiler, A.: Comments on “Homogeneous nucleation rate for highly supercooled cirrus cloud droplets”, *J. Atmos. Sci.*, 46, 2344–2345, doi:10.1175/1520-0469(1989)046<2344:CONRFH>2.0.CO;2, 1989. 1203

## Evaluating ice cloud parameterizations in CAM5

K. Zhang et al.

Title Page

Abstract

Introduction

Conclusions

References

Tables

Figures

◀

▶

◀

▶

Back

Close

Full Screen / Esc

Printer-friendly Version

Interactive Discussion



Diskin, G. S., Podolske, J. R., Sachse, G. W., and Slate, T. A.: Open-path airborne tunable 15 diode laser hygrometer, in: Diode Lasers and Applications in Atmospheric Sensing, edited by: Fried, A., vol. 4187, SPIE Proc., 196–410, 2002. 1205

Earle, M. E., Kuhn, T., Khalizov, A. F., and Sloan, J. J.: Volume nucleation rates for homoge-  
neous freezing in supercooled water microdroplets: results from a combined experimental  
and modelling approach, Atmos. Chem. Phys., 10, 7945–7961, doi:10.5194/acp-10-7945-  
2010, 2010. 1232

Ferrier, B.: A double-moment multiple-phase four-class bulk ice scheme: Part I: Description, J.  
Atmos. Sci., 51, 249–280, 1994. 1211

Field, P. R., Möhler, O., Connolly, P., Krämer, M., Cotton, R., Heymsfield, A. J., Saathoff, H., and  
Schnaiter, M.: Some ice nucleation characteristics of Asian and Saharan desert dust, Atmos.  
Chem. Phys., 6, 2991–3006, doi:10.5194/acp-6-2991-2006, 2006. 1210

Gettelman, A., Morrison, H., and Ghan, S. J.: A new two-moment bulk stratiform cloud micro-  
physics scheme in the Community Atmosphere Model, version 3 (CAM3). Part II: Single-  
column and global results, J. Climate, 21, 3660–3679, doi:10.1175/2008JCLI2116.1, 2008.  
1206

Gettelman, A., Liu, X., Ghan, S. J., Morrison, H., Park, S., Conley, A. J., Klein, S. A., Boyle, J.,  
Mitchell, D. L., and Li, J.-F. L.: Global simulations of ice nucleation and ice supersaturation  
with an improved cloud scheme in the Community Atmosphere Model, J. Geophys. Res.,  
115, D18216, doi:10.1029/2009JD013797, 2010. 1203, 1207, 1208, 1211, 1233

Gettelman, A., Liu, X., Barahona, D., Lohmann, U., and Chen, C.: Climate impacts of ice nucle-  
ation, J. Geophys. Res., 117, D20201, doi:10.1029/2012JD017950, 2012. 1220

Gierens, K.: On the transition between heterogeneous and homogeneous freezing, Atmos.  
Chem. Phys., 3, 437–446, doi:10.5194/acp-3-437-2003, 2003. 1210

Goff, J. A. and Gratch, S.: Low-pressure properties of water from –160 to 212 F, in: Transactions  
of the American Society of Heating and Ventilating Engineers, 52nd Annual Meeting of the  
American Society of Heating and Ventilating Engineers, 95–122, 1946. 1206

Haag, W., Kärcher, B., Ström, J., Minikin, A., Lohmann, U., Ovarlez, J., and Stohl, A.: Freezing  
thresholds and cirrus cloud formation mechanisms inferred from in situ measurements of  
relative humidity, Atmos. Chem. Phys., 3, 1791–1806, doi:10.5194/acp-3-1791-2003, 2003.  
1213

## Evaluating ice cloud parameterizations in CAM5

K. Zhang et al.

Title Page

Abstract

Introduction

Conclusions

References

Tables

Figures

◀

▶

◀

▶

Back

Close

Full Screen / Esc

Printer-friendly Version

Interactive Discussion



Heymsfield, A. J.: Precipitation development in stratiform ice clouds: a micro-physical and dynamical study, *J. Atmos. Sci.*, 34, 367–381, doi:10.1175/1520-0469(1977)034<0367:PDISIC>2.0.CO;2, 1977. 1202

Hoose, C., Kristjánsson, J. E., Chen, J. P., and Hazra, A.: A classical-theory-based parameterization of heterogeneous ice nucleation by mineral dust, soot, and biological particles in a global climate model, *J. Atmos. Sci.*, 67, 2483–2503, doi:10.1175/2010JAS3425.1, 2010. 1203, 1210

Iacono, M., Delamere, J., Mlawer, E., Shephard, M., Clough, S., and Collins, W.: Radiative forcing by long-lived greenhouse gases: calculations with the AER radiative transfer models, *J. Geophys. Res.*, 113, D13103, doi:10.1029/2008JD009944, 2008. 1207

Jensen, E. J. and Toon, O. B.: Ice nucleation in the upper troposphere: sensitivity to aerosol number density, temperature, and cooling rate, *Geophys. Res. Lett.*, 21, 2019–2022, doi:10.1029/94GL01287, 1994. 1232

Jensen, E. J., Toon, O. B., Westphal, D. L., Kinne, S., and Heymsfield, A. J.: Microphysical modeling of cirrus: 2. Sensitivity studies, *J. Geophys. Res.*, 99, 10443–10454, doi:10.1029/94JD00226, 1994. 1220

Jensen, E. J., Toon, O. B., Tabazadeh, A., Sachse, G. W., Anderson, B. E., Chan, K. R., Twohy, C. W., Gandrud, B., Aulenbach, S. M., Heymsfield, A., Hallett, J., and Gary, B.: Ice nucleation processes in upper tropospheric wave-clouds observed during SUCCESS, *Geophys. Res. Lett.*, 25, 1363–1366, doi:10.1029/98GL00299, 1998. 1203

Jensen, E. J., Pfister, L., Bui, T.-P., Lawson, P., and Baumgardner, D.: Ice nucleation and cloud microphysical properties in tropical tropopause layer cirrus, *Atmos. Chem. Phys.*, 10, 1369–1384, doi:10.5194/acp-10-1369-2010, 2010. 1202

Kärcher, B. and Burkhardt, U.: A cirrus cloud scheme for general circulation models, *Q. J. Roy. Meteorol. Soc.*, 134, 1439–1461, doi:10.1002/qj.301, 2008. 1203, 1214

Kärcher, B. and Lohmann, U.: A parameterization of cirrus cloud formation: homogeneous freezing of supercooled aerosols, *J. Geophys. Res.*, 107, D2, doi:10.1029/2001JD000470, 2002. 1232

Kärcher, B. and Lohmann, U.: A parameterization of cirrus cloud formation: heterogeneous freezing, *J. Geophys. Res.-Atmos.*, 108, 4402, doi:10.1029/2002JD003220, 2003. 1220

Kärcher, B. and Spichtinger, B.: Cloud-controlling factors of cirrus, in: *Clouds in the Perturbed Climate System: Their Relationship to Energy Balance, Atmospheric Dynamics, and*

## Evaluating ice cloud parameterizations in CAM5

K. Zhang et al.

Title Page

Abstract

Introduction

Conclusions

References

Tables

Figures

◀

▶

◀

▶

Back

Close

Full Screen / Esc

Printer-friendly Version

Interactive Discussion



Precipitation, edited by: Heintzenberg, J. and Charlson, R. J., vol. 3536, Strüngmann Forum Report, 235–267, The MIT Press, Cambridge, MA, 2009. 1203

Kay, J. E. and Wood, R.: Timescale analysis of aerosol sensitivity during homogeneous freezing and implications for upper tropospheric water vapor budgets, *Geophys. Res. Lett.*, 35, L10809, doi:10.1029/2007GL032628, 2008. 1210

Khorostyanov, V. I. and Sassen, K.: Cirrus cloud simulation using explicit microphysics and radiation. Part I: Model description., *J. Atmos. Sci.*, 55, 1808–1821, doi:10.1175/1520-0469(1998)055<1808:CCSUEM>2.0.CO;2, 1998. 1232

Knollenberg, R. G.: The optical array: an alternative to scattering or extinction for airborne particle size determination, *J. Appl. Meteorol.*, 9, 86–103, 1970. 1205

Koop, T., Luo, B., Tsias, A., and Peter, T.: Water activity as the determinant for homogeneous ice nucleation in aqueous solutions, *Nature*, 406, 611–614, doi:10.1038/35020537, 2000. 1240

Krämer, M., Schiller, C., Afchine, A., Bauer, R., Gensch, I., Mangold, A., Schlicht, S., Spelten, N., Sitnikov, N., Borrmann, S., de Reus, M., and Spichtinger, P.: Ice supersaturations and cirrus cloud crystal numbers, *Atmos. Chem. Phys.*, 9, 3505–3522, doi:10.5194/acp-9-3505-2009, 2009. 1204, 1218

Lamarque, J.-F., Bond, T. C., Eyring, V., Granier, C., Heil, A., Klimont, Z., Lee, D., Liousse, C., Mieville, A., Owen, B., Schultz, M. G., Shindell, D., Smith, S. J., Stehfest, E., Van Aardenne, J., Cooper, O. R., Kainuma, M., Mahowald, N., McConnell, J. R., Naik, V., Riahi, K., and van Vuuren, D. P.: Historical (1850–2000) gridded anthropogenic and biomass burning emissions of reactive gases and aerosols: methodology and application, *Atmos. Chem. Phys.*, 10, 7017–7039, doi:10.5194/acp-10-7017-2010, 2010. 1209

Lawson, R. P.: Effects of ice particles shattering on the 2D-S probe, *Atmos. Meas. Tech.*, 4, 1361–1381, doi:10.5194/amt-4-1361-2011, 2011. 1204, 1205

Lawson, R. P., O'Connor, D., Zmarzly, P., Weaver, K., Baker, B., Mo, Q., and Jonsen, H.: The 2D-S (stereo) probe: design and preliminary tests of a new airborne, high-speed, high-resolution particle imaging probe, *J. Atmos. Ocean. Tech.*, 23, 1462–1477, doi:10.1175/JTECH1927.1, 2006. 1204

Lin, R.-F.: A numerical study of the evolution of nocturnal cirrus by a two-dimensional model with explicit microphysics, PhD thesis, The Pennsylvania State University, Pennsylvania, 199 pp., 1997. 1232

## Evaluating ice cloud parameterizations in CAM5

K. Zhang et al.

Title Page

Abstract

Introduction

Conclusions

References

Tables

Figures

◀

▶

◀

▶

Back

Close

Full Screen / Esc

Printer-friendly Version

Interactive Discussion



- Lin, R. F., Starr, D., DeMott, P., Cotton, R., Sassen, K., Jensen, E., Kärcher, B., and Liu, X.: Cirrus parcel model comparison project. Phase 1: the critical components to simulate cirrus initiation explicitly, *J. Atmos. Sci.*, 59, 2305–2329, doi:10.1175/1520-0469(2002)059<2305:CPMCP>2.0.CO;2, 2002. 1203, 1210, 1232
- 5 Liu, X. and Penner, J.: Ice nucleation parameterization for a global model, *Meteorol. Z.*, 14, 499–514, doi:10.1127/0941-2948/2005/0059, 2005. 1207, 1230, 1231, 1232
- Liu, X. H. and Seidl, W.: Modeling study of cloud droplet nucleation and in-cloud sulfate production during the SANA2 campaign, *J. Geophys. Res.*, 103, 16145–16158, doi:10.1029/98JD00972, 1998. 1232
- 10 Liu, X. H., Penner, J. E., Ghan, S. J., and Wang, M. H.: Inclusion of ice microphysics in the NCAR community atmospheric model version 3 (CAM3), *J. Climate*, 20, 4526–4547, doi:10.1175/JCLI4264.1, 2007. 1203, 1207
- Liu, X., Easter, R. C., Ghan, S. J., Zaveri, R., Rasch, P., Shi, X., Lamarque, J.-F., Gettelman, A., Morrison, H., Vitt, F., Conley, A., Park, S., Neale, R., Hannay, C., Ekman, A. M. L., Hess, P., Mahowald, N., Collins, W., Iacono, M. J., Bretherton, C. S., Flanner, M. G., and Mitchell, D.: Toward a minimal representation of aerosols in climate models: description and evaluation in the Community Atmosphere Model CAM5, *Geosci. Model Dev.*, 5, 709–739, doi:10.5194/gmd-5-709-2012, 2012a. 1207
- 15 Liu, X., Shi, X., Zhang, K., Jensen, E. J., Gettelman, A., Barahona, D., Nenes, A., and Lawson, P.: Sensitivity studies of dust ice nuclei effect on cirrus clouds with the Community Atmosphere Model CAM5, *Atmos. Chem. Phys.*, 12, 12061–12079, doi:10.5194/acp-12-12061-2012, 2012b. 1208, 1211, 1214, 1218
- Lohmann, U. and Hoose, C.: Sensitivity studies of different aerosol indirect effects in mixed-phase clouds, *Atmos. Chem. Phys.*, 9, 8917–8934, doi:10.5194/acp-9-8917-2009, 2009. 1203
- 20 Ulrike Lohmann et al 2008 *Environ. Res. Lett.* 3 045022 doi:10.1088/1748-9326/3/4/045022
- Lohmann, U., Spichtinger, P., Jess, S., Peter, T., and Smit, H.: Cirrus cloud formation and ice supersaturated regions in a global climate model, *Environ. Res. Lett.*, 3, 045022, doi:http://dx.doi.org/10.1088/1748-9326/3/4/045022, 2008. 1203, 1210, 1216
- 30 Mace, G. G., Zhang, Y., Platnick, S., King, M. D., Minnis, P., and Yang, P.: Evaluation of cirrus cloud properties derived from MODIS data using cloud properties derived from ground-

## Evaluating ice cloud parameterizations in CAM5

K. Zhang et al.

Title Page

Abstract

Introduction

Conclusions

References

Tables

Figures

◀

▶

◀

▶

Back

Close

Full Screen / Esc

Printer-friendly Version

Interactive Discussion



based observations collected at the ARM SGP site, *J. Appl. Meteorol.*, 44, 221–240, doi:10.1175/JAM2193.1, 2005. 1204

Magee, N., Moyle, A. M., and Lamb, D.: Experimental determination of the deposition coefficient of small cirrus-like ice crystals near  $-50^{\circ}\text{C}$ , *Geophys. Res. Lett.*, 33, 17, doi:10.1029/2006GL026665, 2006. 1203, 1210, 1215, 1232

Meyers, M. P., Demott, P. J., and Cotton, W. R.: New primary ice-nucleation parameterizations in an explicit cloud model, *J. Appl. Meteorol.*, 31, 708–721, doi:10.1175/1520-0450(1992)031<0708:NPINPI>2.0.CO;2, 1992. 1208, 1230

Mitchell, D.: Effective diameter in radiation transfer: general definition, applications, and limitations, *J. Atmos. Sci.*, 59, 2330–2346, doi:10.1175/1520-0469(2002)059<2330:EDIRTG>2.0.CO;2, 2002. 1206

Mitchell, D. L., Rasch, P., Ivanova, D., McFarquhar, G., and Nousiainen, T.: Impact of small ice crystal assumptions on ice sedimentation rates in cirrus clouds and GCM simulations, *Geophys. Res. Lett.*, 35, 9806, doi:10.1029/2008GL033552, 2008. 1203

Mitchell, D. L., Lawson, R. P., and Baker, B.: Understanding effective diameter and its application to terrestrial radiation in ice clouds, *Atmos. Chem. Phys.*, 11, 3417–3429, doi:10.5194/acp-11-3417-2011, 2011. 1216

Mlawer, E. J., Taubman, S. J., Brown, P. D., Iacono, M. J., and Clough, S. A.: Radiative transfer for inhomogeneous atmospheres: RRTM, a validated correlated- $k$  model for the longwave, *J. Geophys. Res.*, 102, 16663–16682, 1997. 1207

Möhler, O., Field, P. R., Connolly, P., Benz, S., Saathoff, H., Schnaiter, M., Wagner, R., Cotton, R., Krämer, M., Mangold, A., and Heymsfield, A. J.: Efficiency of the deposition mode ice nucleation on mineral dust particles, *Atmos. Chem. Phys.*, 6, 3007–3021, doi:10.5194/acp-6-3007-2006, 2006. 1210

Morrison, H. and Gettelman, A.: A new two-moment bulk stratiform cloud microphysics scheme in the NCAR Community Atmosphere Model (CAM3), Part I: Description and numerical tests, *J. Climate*, 21, 3642–3659, doi:10.1175/2008JCLI2105.1, 2008. 1206, 1207, 1211, 1216, 1219, 1233

Neale, R. B., Chen, C. C., Gettelman, A., Lauritzen, P. H., Park, S., Williamson, D. L., Conley, A. J., Garcia, R., Kinnison, D., Lamarque, J. F., Marsh, D., Mills, M., Smith, A. K., Tilmes, S., Vitt, F., Morrison, H., Cameron-Smith, P., Collins, W. D., Iacono, M. J., Easter, R. C., Ghan, S. J., Liu, X. H., Rasch, P. J., and Taylor, M. A.: Description of the NCAR Community Atmosphere Model (CAM5.0), Tech. Rep. NCAR/TN-486-STR, NCAR,

## Evaluating ice cloud parameterizations in CAM5

K. Zhang et al.

Title Page

Abstract

Introduction

Conclusions

References

Tables

Figures

◀

▶

◀

▶

Back

Close

Full Screen / Esc

Printer-friendly Version

Interactive Discussion



available at: <http://www.cesm.ucar.edu/models/cesm1.0/cam/>, 2010. (last access date: Jan 8, 2013) 1206, 1207, 1214, 1230, 1233

Ovarlez, J., Gayet, J. F., Gierens, K., Stroem, J., Ovarlez, H., Auriol, F., Busen, R., and Schumann, U.: Water vapour measurements inside cirrus clouds in Northern and Southern Hemispheres during INCA, *Geophys. Res. Lett.*, 29, 1813, doi:10.1029/2001GL014440, 2002. 1213

Park, S. and Bretherton, C. S.: The University of Washington shallow convection and moist turbulence schemes and their impact on climate simulations with the Community Atmosphere Model, *J. Climate*, 22, 3449–3469, doi:10.1175/2008JCLI2557.1, 2009. 1207

Park, S., Bretherton, C. S., and Rasch, P. J.: Global cloud simulation in the Community Atmosphere Model 5, *J. Climate*, submitted, 2012. 1206, 1207

Phillips, V. T. J., DeMott, P. J., and Andronache, C.: An empirical parameterization of heterogeneous ice nucleation for multiple chemical species of aerosol, *J. Atmos. Sci.*, 65, 2757–2783, doi:10.1175/2007JAS2546.1, 2008. 1208, 1210

Prenni, A. J., DeMott, P. J., Twohy, C., Poellot, M. R., Kreidenweis, S. M., Rogers, D. C., Brooks, S. D., Richardson, M. S., and Heymsfield, A. J.: Examinations of ice formation processes in Florida cumuli using ice nuclei measurements of anvil ice crystal particle residues, *J. Geophys. Res.-Atmos.*, 112, 10221, doi:10.1029/2006JD007549, 2007. 1203

Pruppacher, H. R. and Klett, J. D.: *Microphysics of Clouds and Precipitation*, 2nd edn., Springer, New York, 1997. 1210

Richter, J. H. and Rasch, P. J.: Effects of convective momentum transport on the atmospheric circulation in the community atmosphere model, version 3, *J. Climate*, 21, 1487–1499, doi:10.1175/2007JCLI1789.1, 2008. 1207

Salzmann, M., Ming, Y., Golaz, J.-C., Ginoux, P. A., Morrison, H., Gettelman, A., Krämer, M., and Donner, L. J.: Two-moment bulk stratiform cloud microphysics in the GFDL AM3 GCM: description, evaluation, and sensitivity tests, *Atmos. Chem. Phys.*, 10, 8037–8064, doi:10.5194/acp-10-8037-2010, 2010. 1203

Sassen, K. and Dodd, G. C.: Homogeneous nucleation rate for highly supercooled cirrus cloud droplets, *J. Atmos. Sci.*, 45, 1357–1369, doi:10.1175/1520-0469(1988)045<1357:HNRFHS>2.0.CO;2, 1988. 1203, 1232

Skrotzki, J., Connolly, P., Schnaiter, M., Saathoff, H., Möhler, O., Wagner, R., Niemand, M., Ebert, V., and Leisner, T.: The accommodation coefficient of water molecules on ice-cirrus

**Evaluating ice cloud  
parameterizations in  
CAM5**

K. Zhang et al.

Title Page

Abstract

Introduction

Conclusions

References

Tables

Figures

◀

▶

◀

▶

Back

Close

Full Screen / Esc

Printer-friendly Version

Interactive Discussion



cloud studies at the AIDA simulation chamber, *Atmos. Chem. Phys. Discuss.*, 12, 24351–24393, doi:10.5194/acpd-12-24351-2012, 2012. 1232

Smith, W. L., Ackerman, S., Revercomb, H., Huang, H., DeSlover, D. H., Feltz, W., Gumley, L., and Collard, A.: Infrared spectral absorption of nearly invisible cirrus clouds, *Geophys. Res. Lett.*, 25, 1137–1140, doi:10.1029/97GL03491, 1998. 1202

Spice, A., Johnson, D. W., Brown, P. R. A., Darlison, A. G., and Saunders, C. P. R.: Primary ice nucleation in orographic cirrus clouds: a numerical simulation of the microphysics, *Q. J. Roy. Meteorol. Soc.*, 125, 1637–1667, doi:10.1002/qj.49712555708, 1999. 1232

Spichtinger, P. and Gierens, K. M.: Modelling of cirrus clouds – Part 2: Competition of different nucleation mechanisms, *Atmos. Chem. Phys.*, 9, 2319–2334, doi:10.5194/acp-9-2319-2009, 2009. 1203

Spichtinger, P., Gierens, K., Smit, H. G. J., Ovarlez, J., and Gayet, J.-F.: On the distribution of relative humidity in cirrus clouds, *Atmos. Chem. Phys.*, 4, 639–647, doi:10.5194/acp-4-639-2004, 2004. 1213

Tabazadeh, A., Martin, S. T., and Lin, J.-S.: The effect of particle size and nitric acid uptake on the homogeneous freezing of aqueous sulfuric acid particles, *Geophys. Res. Lett.*, 27, 1111–1114, doi:10.1029/1999GL010966, 2000. 1232

Wang, M. and Penner, J. E.: Cirrus clouds in a global climate model with a statistical cirrus cloud scheme, *Atmos. Chem. Phys.*, 10, 5449–5474, doi:10.5194/acp-10-5449-2010, 2010. 1203, 1214

Young, K.: A numerical simulation of wintertime, orographic precipitation. Part I: Description of model microphysics and numerical technique, *J. Atmos. Sci.*, 31, 1735–1748, doi:10.1175/1520-0469(1974)031<1735:ANSOWO>2.0.CO;2, 1974. 1208, 1230

Yun, Y. and Penner, J. E.: Global model comparison of heterogeneous ice nucleation parameterizations in mixed phase clouds, *J. Geophys. Res.*, 117, 7203, doi:10.1029/2011JD016506, 2012. 1203

Zhang, G. J. and McFarlane, N. A.: Sensitivity of climate simulations to the parameterization of cumulus convection in the Canadian Climate Centre general circulation model, *Atmos.-Ocean*, 33, 407–446, 1995. 1207

## Evaluating ice cloud parameterizations in CAM5

K. Zhang et al.

**Table 1.** Number of measurement samples obtained inside and outside synoptic cirrus clouds during the SPARTICUS campaign in a 600 km × 600 km area centered at the ARM SGP site (cf. Fig. 1). When the ice crystal number concentration ( $N_i$ ) is larger than 0.01 L<sup>-1</sup>, it is considered as inside cirrus.

Temperature range	Inside cirrus	Outside cirrus
205 K–215 K	11 926	9719
215 K–225 K	32 627	26 076
225 K–235 K	35 935	23 957
235 K–245 K	18 480	15 719

Title Page

Abstract

Introduction

Conclusions

References

Tables

Figures

◀

▶

◀

▶

Back

Close

Full Screen / Esc

Printer-friendly Version

Interactive Discussion



## Evaluating ice cloud parameterizations in CAM5

K. Zhang et al.

**Table 2.** Ice formation mechanisms considered in the CAM5 model (version CAM5.0\_40) and the ambient conditions under which they can take effect.  $q_1$  and  $N(D_p)$  denote the mass mixing ratio and size distribution function of cloud droplets, respectively.  $T_m$  (unit: °C) is the equivalent temperature defined in Liu and Penner (2005, LP05).  $RH_w^{cr}$  denotes the critical relative humidity with respect to water for homogeneous nucleation.

Mechanisms	Condition	Initial crystal size	Reference
In-situ nucleation in cirrus clouds	$-37^\circ\text{C} < T < 0^\circ\text{C}$ and $q_1 = 0$ , or $T < -37^\circ\text{C}$		
Option 1: LP05 scheme			Liu and Penner (2005)
Homogeneous nucleation	$T < T_m - 5$ , $RH_w > RH_w^{cr}$	10 $\mu\text{m}$	
Heterogeneous nucleation	$T_m < T < 0^\circ\text{C}$ , $RH_i > 120\%$	10 $\mu\text{m}$	
Transition (Hom/Het) nucleation	$T_m - 5 < T < T_m$ , $RH_i > 120\%$	10 $\mu\text{m}$	
Option 2: BN09 scheme			Barahona and Nenes (2008, 2009b)
Homogeneous nucleation	$T < -37^\circ\text{C}$ , $RH_w > RH_w^{cr}$	10 $\mu\text{m}$	
Heterogeneous nucleation	$T < 0^\circ\text{C}$ , $RH_i > 120\%$	10 $\mu\text{m}$	
In situ formation in mixed-phase clouds	$q_1 > 0$ and $T < 0^\circ\text{C}$		
Contact freezing	$T < -4^\circ\text{C}$	Dependent on $N(D_p)$	Young (1974)
Deposition/condensation freezing	$-37^\circ\text{C} < T < 0^\circ\text{C}$	10 $\mu\text{m}$	Meyers et al. (1992)
Homogeneous freezing of cloud droplets	$T < -40^\circ\text{C}$	25 $\mu\text{m}$	
Detrainment from convective clouds			
Shallow convection	$T < -5^\circ\text{C}$	50 $\mu\text{m}$	Neale et al. (2010)
Deep convection	$T < -5^\circ\text{C}$	25 $\mu\text{m}$	

[Title Page](#)
[Abstract](#)
[Introduction](#)
[Conclusions](#)
[References](#)
[Tables](#)
[Figures](#)
[Back](#)
[Close](#)
[Full Screen / Esc](#)
[Printer-friendly Version](#)
[Interactive Discussion](#)


**Table 3.** List of sensitivity experiments presented in this study.

Experiment name	Purpose and configuration
Group A:	Sensitivity to nucleation scheme for cirrus clouds
LP	Liu and Penner (2005) scheme for in situ ice nucleation in cirrus cloud, freezing of droplets in mixed phase clouds considered. With deposition coefficient of $\alpha = 0.1$ and $D_{cs} = 400 \mu\text{m}$ .
LPHET	As in LP, but only with heterogeneous nucleation in cirrus clouds.
LPHOM	As in LP, but only with homogeneous nucleation in cirrus clouds.
BN	Barahona and Nenes (2009b) scheme for in situ ice nucleation in cirrus cloud, IN spectra follows Philips et al. (2008), with deposition coefficient of $\alpha = 0.1$ and $D_{cs} = 400 \mu\text{m}$ .
BNHET	As in BN, but only with heterogeneous nucleation in cirrus clouds.
BNHOM	As in BN, but only with homogeneous nucleation in cirrus clouds.
Group B:	Sensitivity to the max freezing ratio of aerosols ( $f_{max}$ )
BNCNT	As in BN in Group A, but uses a classical nucleation theory (CNT) based IN spectra for heterogeneous nucleation in the ice phase. With $\alpha = 0.1$ , $D_{cs} = 400 \mu\text{m}$ , and $f_{max} = 5\%$ .
BNCNT_F10	As in BNCNT, but with $f_{max} = 10\%$ .
BNCNT_F50	As in BNCNT, but with $f_{max} = 50\%$ .
BNCNT_F100	As in BNCNT, but with $f_{max} = 100\%$ .
Group C:	Sensitivity to the water vapor deposition coefficient $\alpha$ (default value = 0.1)
BN_α0.5	As in BN of Group A, but with $\alpha = 0.5$
BN_α0.05	As in BN of Group A, but with $\alpha = 0.05$
BN_α0.006	As in BN of Group A, but with $\alpha = 0.006$
Group D:	Sensitivity to crystal/snow separating diameter $D_{cs}$ (default value = 400 $\mu\text{m}$ )
BN_Dcs175	As in BN of Group A, but with $D_{cs} = 175 \mu\text{m}$
BN_Dcs250	As in BN of Group A, but with $D_{cs} = 250 \mu\text{m}$
BN_Dcs325	As in BN of Group A, but with $D_{cs} = 325 \mu\text{m}$

## Evaluating ice cloud parameterizations in CAM5

K. Zhang et al.

Title Page

Abstract

Introduction

Conclusions

References

Tables

Figures

◀

▶

◀

▶

Back

Close

Full Screen / Esc

Printer-friendly Version

Interactive Discussion



## Evaluating ice cloud parameterizations in CAM5

K. Zhang et al.

Title Page

Abstract

Introduction

Conclusions

References

Tables

Figures

◀

▶

◀

▶

Back

Close

Full Screen / Esc

Printer-friendly Version

Interactive Discussion



**Table 4.** Range of deposition coefficient ( $\alpha$ ) derived from laboratory experiment and field measurements as well as those used in cirrus parcel models and GCM parameterizations. Values for parcel models are collected from Lin et al. (2002). Values from Pruppacher and Klett (1997) are collected from their Table 5.5.

$\alpha$	Reference
Experimentally determined values	
0.006	Magee et al. (2006)
0.014–1.0	Pruppacher and Klett (1997)
$0.031 \pm 0.001$	Earle et al. (2010)
$0.6 \pm 0.2$	Skrotzki et al. (2012)
Values used in parcel models or GCM parameterizations	
0.04	DeMott et al. (1994) and DeMott et al. (1998)
0.1	Lin (1997); Liu and Seidl (1998); Liu and Penner (2005), Barahona and Nenes (2008)
0.24	Spice et al. (1999)
0.36	Sassen and Dodd (1988) and Khvorostyanov and Sassen (1998)
0.5	Kärcher and Lohmann (2002)
1.0	Jensen and Toon (1994) and Tabazadeh et al. (2000)

## Evaluating ice cloud parameterizations in CAM5

K. Zhang et al.

Title Page

Abstract

Introduction

Conclusions

References

Tables

Figures

◀

▶

◀

▶

Back

Close

Full Screen / Esc

Printer-friendly Version

Interactive Discussion



**Table 5.** Values of  $D_{cs}$  (unit:  $\mu\text{m}$ ) in different versions of the CAM5 model.  $D_{cs}$  is the prescribed separating size that distinguishes cloud ice and snow as two different classes of solid-phase condensates.

$D_{cs}$ ( $\mu\text{m}$ )	Reference
200	Morrison and Gettelman (2008)
250	Gettelman et al. (2010)
325	CAM5.0, Neale et al. (2010)
400	CAM5.1, <a href="http://www.cesm.ucar.edu/models/cesm1.0/cam/">http://www.cesm.ucar.edu/models/cesm1.0/cam/</a>



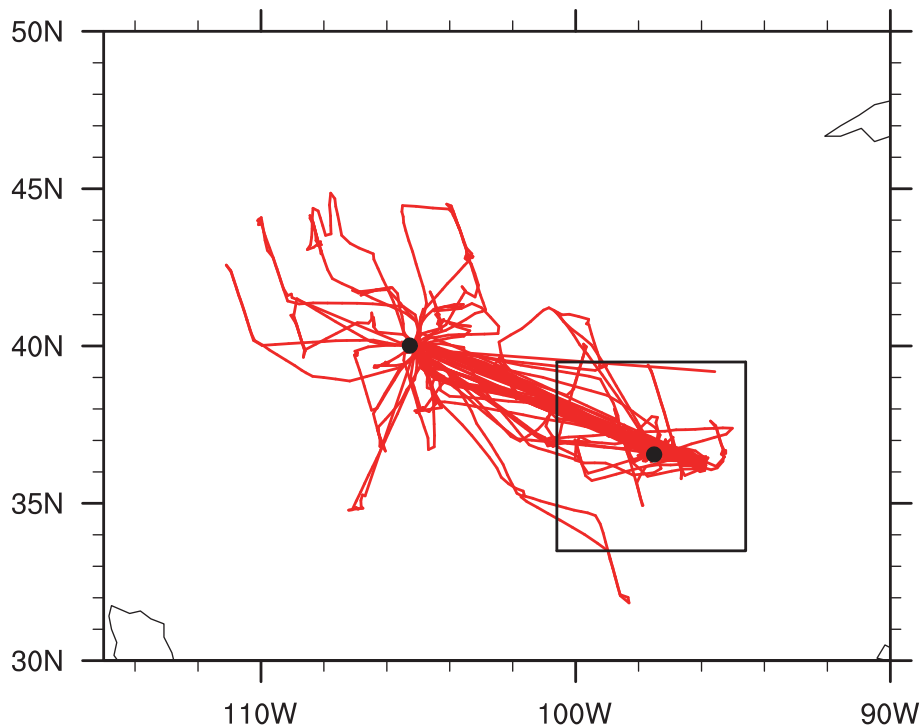


**Fig. 1.** Aircraft trajectories during the SPARTICUS field campaign. The black dot at 40° N shows the location of Boulder, CO. The square indicates a 6° × 6° (about 600 km × 600 km) area centered at the ARM SGP site (36° N, 97° W), within which the ice crystal number measurements are used for model evaluation in this paper. Further details can be found in Sect. 2

**Evaluating ice cloud parameterizations in CAM5**

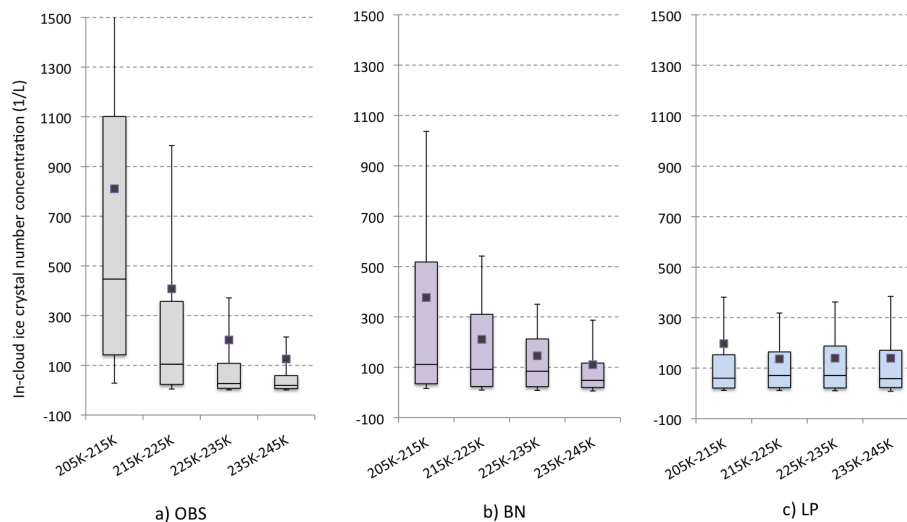
K. Zhang et al.

<a href="#">Title Page</a>	
<a href="#">Abstract</a>	<a href="#">Introduction</a>
<a href="#">Conclusions</a>	<a href="#">References</a>
<a href="#">Tables</a>	<a href="#">Figures</a>
<a href="#">◀</a>	<a href="#">▶</a>
<a href="#">◀</a>	<a href="#">▶</a>
<a href="#">Back</a>	<a href="#">Close</a>
<a href="#">Full Screen / Esc</a>	
<a href="#">Printer-friendly Version</a>	
<a href="#">Interactive Discussion</a>	



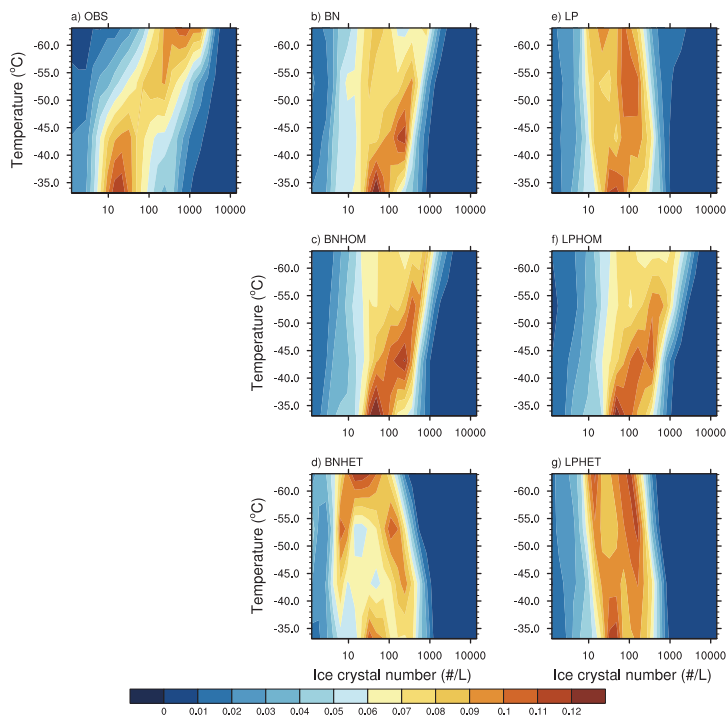
## Evaluating ice cloud parameterizations in CAM5

K. Zhang et al.



**Fig. 2.** Box plots showing the observed and simulated in-cirrus ice crystal number concentration (unit:  $L^{-1}$ ) in the upper troposphere (above 500 hPa) over the SGP area. LP and BN refer to simulations performed with different ice nucleation parameterizations for cirrus clouds (cf. Table 3, Group A). The two whiskers of each box denote the 10th (lower) and 90th (upper) percentiles. Hinges from bottom to top are the 25th, 50th, and 75th percentiles, respectively. Filled squares denote the mean values. The observed 90th percentile ( $1981 L^{-1}$ ) goes off chart (a).

[Title Page](#)
[Abstract](#)
[Introduction](#)
[Conclusions](#)
[References](#)
[Tables](#)
[Figures](#)
[◀](#)
[▶](#)
[◀](#)
[▶](#)
[Back](#)
[Close](#)
[Full Screen / Esc](#)
[Printer-friendly Version](#)
[Interactive Discussion](#)

**Fig. 3.** Observed and simulated Probability Density Function (PDF) of ice crystal number concentration in cirrus clouds in the upper troposphere (above 500 hPa) at different ambient temperatures. The observed PDF is derived from 1 Hz measurements in the SGP area obtained during the SPARTICUS campaign. The simulated PDFs are computed from five years of instantaneous 3-hourly model output in the months and locations of the measurements.

## Evaluating ice cloud parameterizations in CAM5

K. Zhang et al.

Title Page

Abstract

Introduction

Conclusions

References

Tables

Figures

◀

▶

◀

▶

Back

Close

Full Screen / Esc

Printer-friendly Version

Interactive Discussion



## Evaluating ice cloud parameterizations in CAM5

K. Zhang et al.

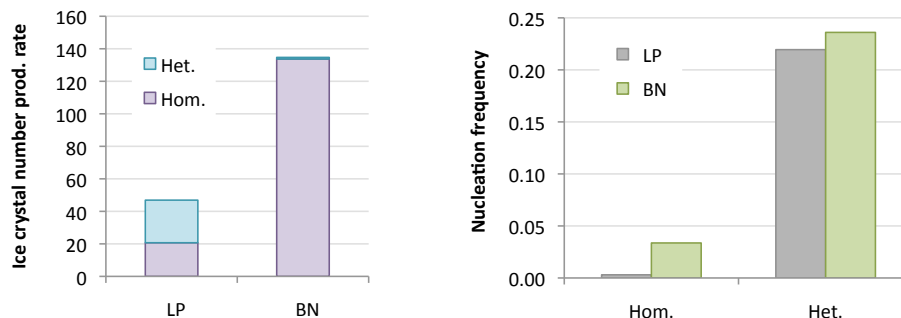


**Fig. 4.** Left: contributions of heterogeneous and homogeneous ice nucleation to crystal production at 200 hPa over the SGP area in CAM5 simulations performed with the default LP05 and BN09 parameterization schemes (cf. Table 3, Group A). The production rates are given in the unit of number of crystals per liter per model time step (i.e. 30 min). Right: the frequency of occurrence of the two nucleation mechanisms in different simulations.

[Title Page](#)[Abstract](#)[Introduction](#)[Conclusions](#)[References](#)[Tables](#)[Figures](#)[◀](#)[▶](#)[◀](#)[▶](#)[Back](#)[Close](#)[Full Screen / Esc](#)[Printer-friendly Version](#)[Interactive Discussion](#)

**Evaluating ice cloud  
parameterizations in  
CAM5**

K. Zhang et al.

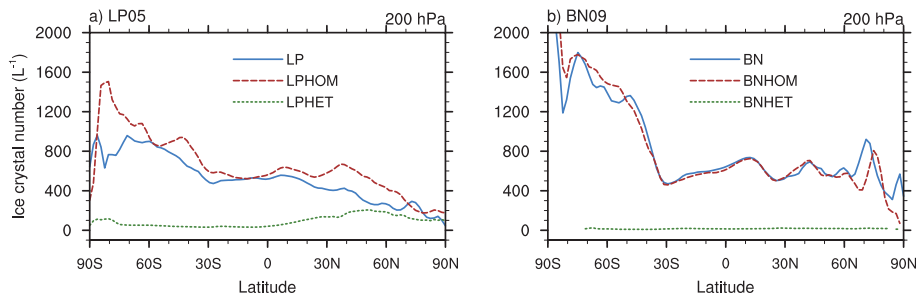


**Fig. 5.** Zonally and annually averaged 200 hPa in-cirrus ice crystal number concentration (unit:  $L^{-1}$ ) simulated with different ice nucleations schemes. The simulations correspond to Group A in Table 2.

[Title Page](#)[Abstract](#)[Introduction](#)[Conclusions](#)[References](#)[Tables](#)[Figures](#)[◀](#)[▶](#)[◀](#)[▶](#)[Back](#)[Close](#)[Full Screen / Esc](#)[Printer-friendly Version](#)[Interactive Discussion](#)

## Evaluating ice cloud parameterizations in CAM5

K. Zhang et al.

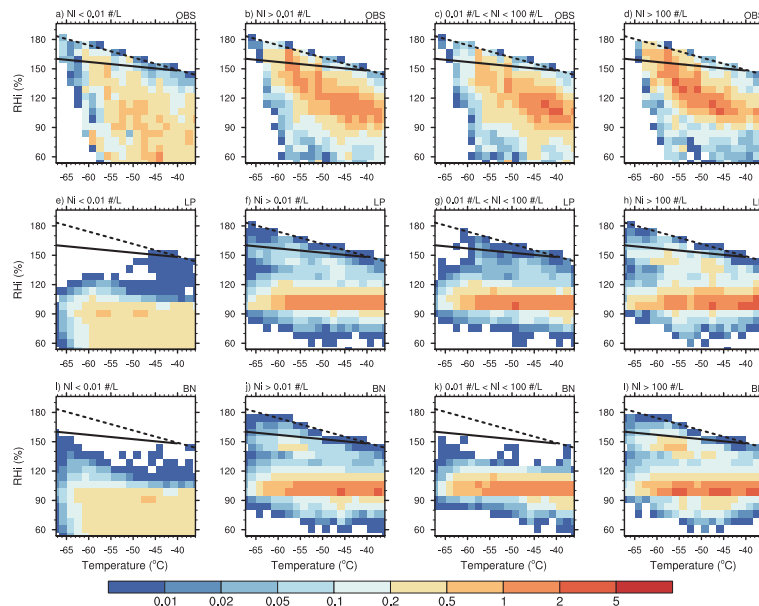


**Fig. 6.** Observed and simulated joint probability density function (PDF) of relative humidity with respect to ice ( $RH_i$ , unit: %) and ambient temperature (unit:  $^{\circ}\text{C}$ ) in the upper troposphere (above 500 hPa), in clear-sky conditions ( $N_i < 0.01 \text{ L}^{-1}$ , first column) and inside cirrus clouds ( $N_i > 0.01 \text{ L}^{-1}$ , second column). The in-cirrus cases are further divided into two sub-groups with different ice crystal number concentration ranges:  $0.01 \text{ L}^{-1} < N_i < 100 \text{ L}^{-1}$  (third column) and  $N_i > 100 \text{ L}^{-1}$  (rightmost column). The observed PDF is derived from 1 Hz measurements in the SGP area obtained during the SPARTICUS campaign. The simulated PDFs are computed from five years of instantaneous 3-hourly model output in the SGP area (cf. Fig. 1) in the months when the measurements were taken. The dashed line indicates water saturation. The solid black line is the homogeneous freezing threshold for liquid solution droplets with  $0.5 \mu\text{m}$  radius calculated according to Koop et al. (2000).

Title Page

Abstract

Introduction

Conclusions

References

Tables

Figures

◀

▶

◀

▶

Back

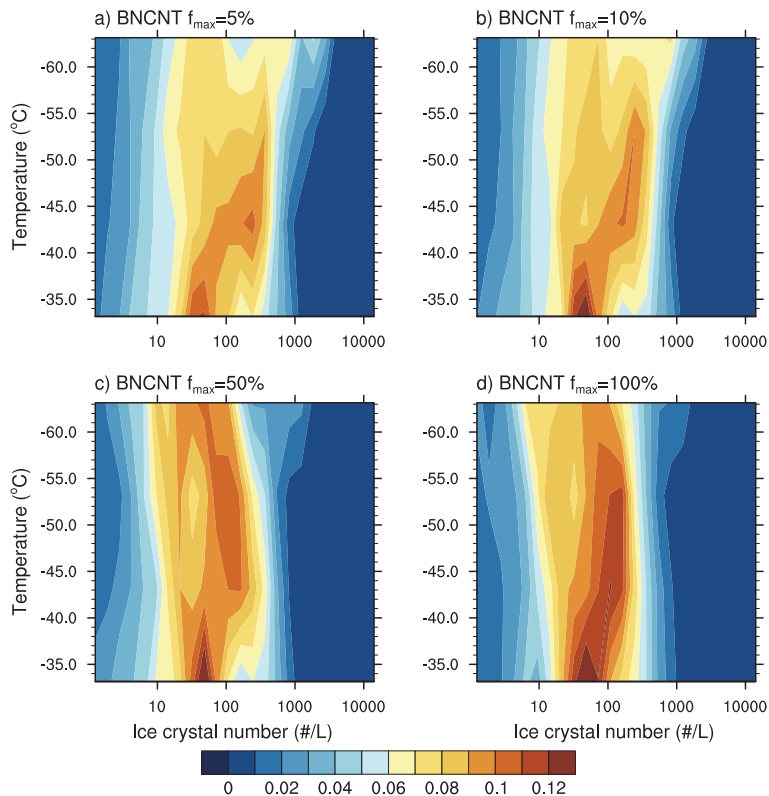
Close

Full Screen / Esc

Printer-friendly Version

Interactive Discussion

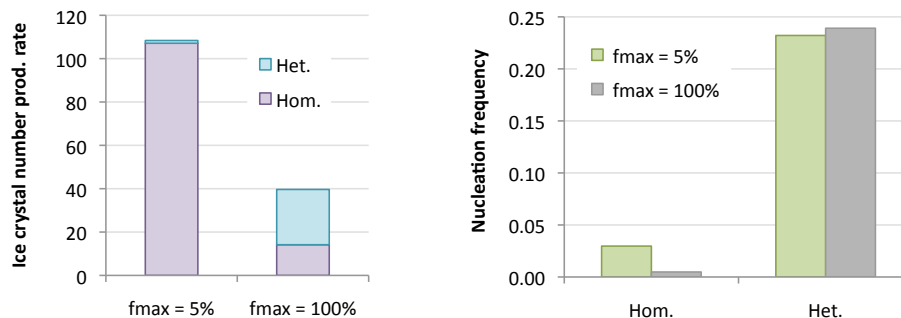




**Fig. 7.** As in Fig. 3 but for simulations in Group B. The simulations are performed with the BN09 ice nucleation scheme with a classical-theory-based IN spectra and different values for the maximum freezing ratio of potential ice nuclei ( $f_{max}$ ). Further details can be found in Table 3 (Group B) and Sect. 5.2.

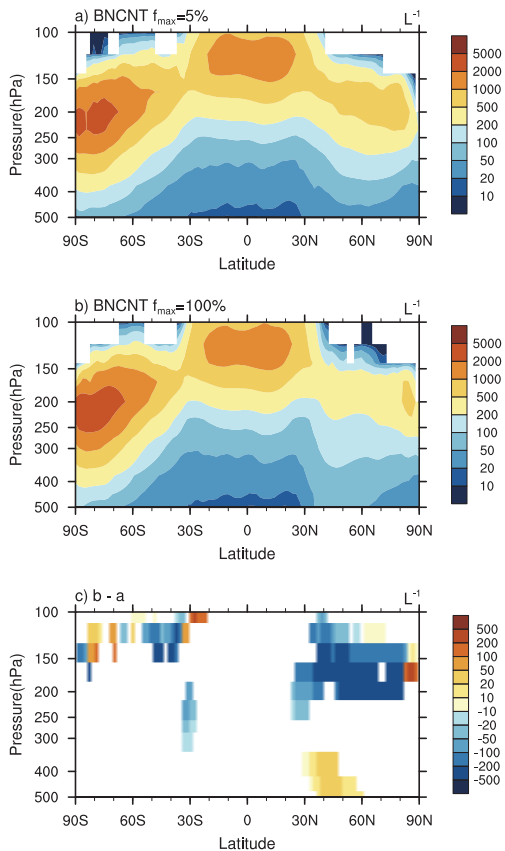
## Evaluating ice cloud parameterizations in CAM5

K. Zhang et al.



**Fig. 8.** As in Fig. 4, but comparing two simulations performed with the BN09 ice nucleation scheme using a classical-theory-based IN spectra and different values for the maximum freezing ratio of potential ice nuclei ( $f_{\max}$ ). Further details can be found in Table 3 (Group B) and Sect. 5.2.

[Title Page](#)
[Abstract](#)
[Introduction](#)
[Conclusions](#)
[References](#)
[Tables](#)
[Figures](#)
[◀](#)
[▶](#)
[◀](#)
[▶](#)
[Back](#)
[Close](#)
[Full Screen / Esc](#)
[Printer-friendly Version](#)
[Interactive Discussion](#)

**Fig. 9.** Annually and zonally averaged in-cloud ice crystal number concentration ( $L^{-1}$ ) simulated with the BN09 ice nucleation scheme using a classical-theory-based IN spectra and different values for the maximum freezing ratio of potential ice nuclei ( $f_{max}$ ). Further details can be found in Table 3 (Group B) and Sect. 5.2.

**Evaluating ice cloud parameterizations in CAM5**

K. Zhang et al.

Title Page

Abstract

Introduction

Conclusions

References

Tables

Figures

◀

▶

◀

▶

Back

Close

Full Screen / Esc

Printer-friendly Version

Interactive Discussion



**Evaluating ice cloud parameterizations in CAM5**

K. Zhang et al.

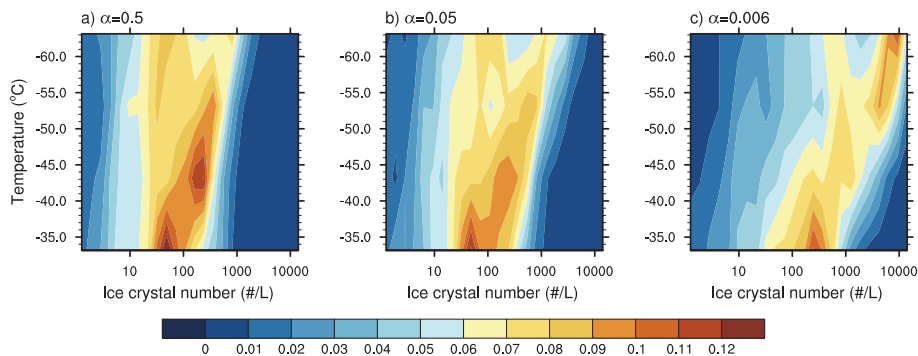


**Fig. 10.** As in Fig. 3 but for simulations in Group C. Further details can be found in Table 3 and Sect. 5.3.

Title Page

Abstract

Introduction

Conclusions

References

Tables

Figures

◀

▶

◀

▶

Back

Close

Full Screen / Esc

Printer-friendly Version

Interactive Discussion



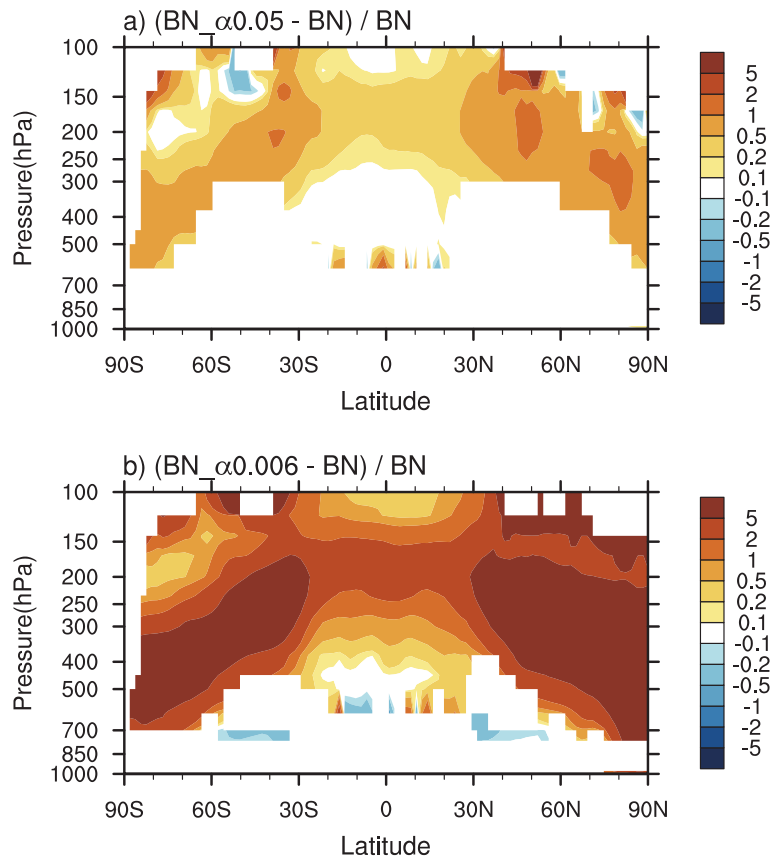


**Fig. 11.** Relative differences in the zonally and annually averaged in-cloud ice crystal number concentration between simulations that use different water vapor deposition coefficient ( $\alpha$ ) in the BN09 ice nucleation scheme.

## Evaluating ice cloud parameterizations in CAM5

K. Zhang et al.

Title Page

Abstract

Introduction

Conclusions

References

Tables

Figures

◀

▶

◀

▶

Back

Close

Full Screen / Esc

Printer-friendly Version

Interactive Discussion



**Evaluating ice cloud  
parameterizations in  
CAM5**

K. Zhang et al.

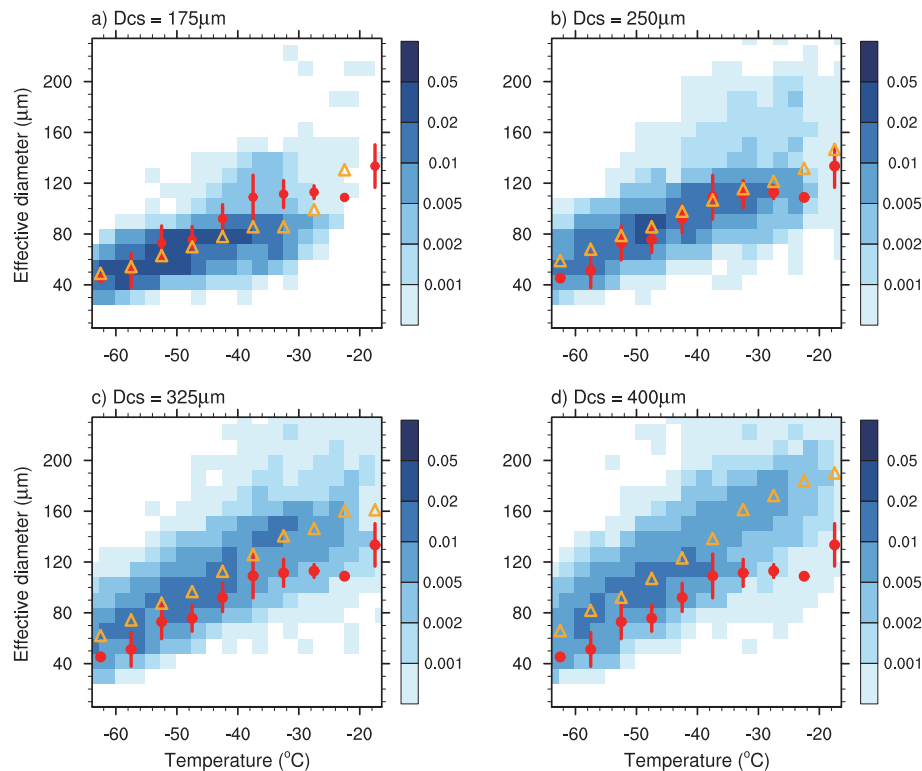


**Fig. 12.** Color shading shows the bi-variable PDF of temperature and the effective diameter of ice crystals simulated with CAM5 using different values of the parameter  $D_{cs}$ . Triangles indicate the simulated mean effective diameter at different temperatures. The red dots and whiskers indicate the mean and standard deviation derived from the SPARTICUS measurements.

Title Page

Abstract

Introduction

Conclusions

References

Tables

Figures

◀

▶

◀

▶

Back

Close

Full Screen / Esc

Printer-friendly Version

Interactive Discussion

